The Effects of 1-(5-Iodonaphthalene-1-sulfonyl)-1H-hexahydro-1,4-diazepine hydrochloride (ML-7) on the Lens During Avian Accommodation *In Situ*

by

Sara Luck

A thesis
presented to the University of Waterloo
in fulfillment of the
thesis requirement for the degree of
Master of Science
in
Vision Science and Biology

Waterloo, Ontario, Canada, 2009

AUTHOR'S DECLARATION

I hereby declare that I am the sole author of this thesis. This is a true copy of the thesis, including any required final revisions, as accepted by my examiners.

I understand that my thesis may be made electronically available to the public.

Abstract

A previous study in chickens revealed that myosin light chain kinase (MLCK), f-actin, and myosin are found on the crystalline lens. Their polygonal arrangement at the posterior surface resembles a muscle tissue, which suggests that these proteins may have a contractile role in accommodation. The ciliary muscle in chickens is skeletal in nature and, therefore, chickens were used to test the hypothesis that contractile microfilaments play a role in accommodation. Ciliary nerve-induced accommodation was measured in the presence of an MLCK inhibitor 1-(5-Iodonaphthalene-1-sulfonyl)-1H-hexahydro-1,4-diazepine hydrochloride (ML-7).

Eyes of 6-day old white Leghorn chickens (*gallus gallus domesticus*) were enucleated in Tyrode's saline solution while keeping the ciliary nerve intact. One eye was treated with ML-7 and the other eye was treated with vehicle only. Three concentrations of ML-7 were used: 1 μM, 10 μM, and 100 μM. Two experiments were carried out, one including a (3×10 min) wash and one without. Focal lengths of the vehicle- and ML-7-treated eyes were measured before, during and after accommodation. Immunoblots were used to detect the amount of phosphorylated myosin with and without the inhibitor.

Focal lengths for accommodation were shorter than those at rest ($p<0.001$). In the wash experiment, vehicle-treated eyes had higher accommodative amplitudes compared to ML-7-treated eyes for all three dosage groups. In the no-wash experiment, only the 1 μM group demonstrated the same trend as the wash experiment. For the 10 μM and 100 μM groups, ML-7-treated eyes had higher accommodative amplitudes compared to vehicle-treated eyes. Immunoblots revealed varying amounts of inhibition within pairs of eyes as

well as between birds for both experiments. Results from this experiment indicate that ML-7 was not effective at determining whether contractile microfilaments found on the lens contribute to accommodation.

Acknowledgements

First, I would like to acknowledge my supervisor Dr. Vivian Choh for being a great mentor and taking the time to teach me dissections, statistics, keyboard shortcuts and much more. I could not have successfully completed my degree without her. I would like to thank my committee members, Dr. Jake Sivak, for his helpful guidance, lab space and equipment and Dr. Matt Vijayan for his expert advice and suggestions.

Thanks to my many lab mates starting with the original Viv's chicks, Jackie Fleming and Christina Vesco; the Leak Patrol team, Katie Mazurewicz, Stacey Chong and Lisa Pray; Liem Ho for helping me get the project started and Angela Backman for helping me finish it. Thanks to the Lego team, Derek Ho, Raiju Babu and Krithika Nandakumar, you made this experience so very memorable. I would like thank Elizabeth Joyce and Miriam Heynen for teaching me how to run a Western blot. Thanks to Nancy MacNeil for making TAing enjoyable. I would also like to thank Daniel Williams for his continual support and computer skills.

I would like to thank Maple Leaf Poultry, for supplying the chickens needed for this research to take place and Nancy Gibson for taking care of the chickens. Thanks to the Sivak lab for sharing their lab space. Special thanks to Dr. Tom Singer for allowing me to volunteer in his lab and introducing me to the world of vision science research. To all my fellow graduate students, faculty and staff, thank you for making this experience wonderful.

Finally, I would also like to acknowledge the Natural Sciences and Engineering Research Council (NSERC) of Canada and the Canadian Optometric Education Trust Fund (COETF) for funding this project.

Dedication

My thesis is dedicated to my family.

Thank you for believing in me and supporting me every step of the way.

Table of Contents

List of Figures

List of Tables

List of Abbreviations/Acronyms

µL	microlitre(s)
µg	microgram(s)
ADP	adenosine diphosphate
ANOVA	analysis of variance
ATP	adenosine triphosphate
BB	blocking buffer
BioStab	BioStab™ biomolecule storage solution
BSA	bovine serum albumin
BVFL	back vertex focal length
D	dioptre(s)
EtOH	ethanol
g	force of gravity
GLB	gel loading buffer
Hz	hertz
IC_{50}	$_{h}$alf maximal inhibitory concentration
kDa	kilodaltons
mA	milliampere(s)
min	minute(s)
mL	milliliters
MLC	myosin light chain
MLCK	myosin light chain kinase
ML-7	1-(5-Iodonaphthalene-1-sulfonyl)-1H-hexahydro-1,4-diazepine hydrochloride

ML-9	1-(5-Chloronaphthalene-1-sulfonyl)-1H-hexahydro-1,4-diazepine hydrochloride
mm	millimeter(s)
mM	millimolar
Pi	inorganic phosphate
PBS	Phosphate Buffered Saline
PBST	Phosphate Buffered Saline Tween-20
PVDF	polyvinylidene difluoride
s.d.	standard deviation
SDS	sodium dodecyl sulphate
s.e.m	standard error of the mean
Tris	tris (hydroxylmethyl) aminomethane
TS	Tyrodes's Solution
v/v	volume/volume
w/v	weight/volume
×	times, by
^{o}C	degrees Celsius

I. Introduction

The lens provides one third of the eye's total dioptric power (Schwartz, 1994). The lens, along with the cornea, is responsible for focusing nearby objects onto the retina, in a process called accommodation. In humans, accommodation is a cascade of events involving ciliary muscle contraction, reduction in the tension of the zonules and finally, a change of the lens shape so that its surfaces are more curved, resulting in a higher refractive power (Remington, 2005).

Cellular movements are known to occur when there is a presence of both actin and myosin. Their interactions make a molecular motor, which is found in muscle tissue as well as in non-muscle tissue. Previous studies revealed that the anterior epithelium of the lens has a network of filamentous f-actin polygonal arrays that are colocalised with myosin (Rafferty *et al.*, 1990, Rafferty *et al.*, 1994). A similar arrangement of actin and myosin was observed at the posterior surface on the capsule in chicken lenses, along with other proteins, such as N-cadherin, myosin light chain kinase (MLCK), and additional proteins that are involved in contraction (Bassnett *et al.*, 1999). Both investigating groups report that the cytoskeletal protein arrays resemble a contractile system. Together, these studies suggest that the subcellular cytoskeletal proteins within the lens might play a role in contraction and therefore accommodation of the lens.

The purpose of this study was to determine whether the contractile proteins found on the lens play a significant role in accommodation. Since MLCK is found on the lens, an MLCK inhibitor, such as 1-(5-Iodonaphthalene-1-sulfonyl)-1H-hexahydro-1,4-diazepine hydrochloride (ML-7), would be expected to disrupt any potential actin-myosin interactions

on the lens. It is known that MLCK phosphorylates myosin light chain, which activates actin and myosin contraction in smooth muscle. Therefore, inhibiting MLCK on the lens would interfere with the possible contraction that is taking place, resulting in a change in accommodative amplitude.

II. Literature Review

2.1 The Crystalline Lens

2.1.1 Role of the crystalline lens

The lens is an isolated organ that plays a significant role in vision (Obrecht and Stark, 1991). Its optical function, along with the cornea, is to focus images on the retina. In order for the lens to function properly, it must be transparent, have a high index of refraction and be able to accommodate (Mathias *et al.*, 1997).

2.1.2 Embryological development

Lens development begins by a number of inductive interactions within the embryo. The vertebrate eye develops from three primordial tissues; these include neural ectoderm, surface ectoderm and mesoderm (Gwon, 2006). The lens is derived from the surface ectoderm. Lens development starts when the optic vesicle evaginates from the brain and grows towards the surface ectoderm (Gilbert, 1994). Both the optic vesicle and the surface ectoderm then thicken by the elongation and proliferation of the cells, forming the optic cup and the lens placode, respectively. The lens placode, the area of thickened columnar cells, then buckles inward creating a lens pit that folds inward within the optic cup. Eventually, the lens pit turns into a complete hollow sphere of epithelial lens cells that pinches off of the surface ectoderm. The optic cup becomes the neural and pigmented retina. The posterior epithelial cells elongate into fibres uni-directionally into the lumen of the lens (Kuwabara, 1975; Oyster, 1999) and eliminating their cell nuclei. The cells continue to elongate until they reach the posterior edge of the anterior epithelial cells. These fibre cells that fill the

lumen of the lens vesicle are known as the primary fibres. The primary fibres make up the embryonic nucleus, which is the oldest part of the lens (Cohen, 1965).

The epithelial cells are the progenitors of the adult lens. They persist as a monolayer at the anterior of the lens. The germinative zone lies near the equator of the lens; this is the location where anterior epithelial cells proliferate. From the germinative zone, cells migrate slightly posteriorly, before elongating bi-directionally. As these fibres, called secondary fibres, elongate, the anterior end is situated between the lens epithelium and the primary fibres, while the posterior end is situated between the primary fibres and the posterior capsule. Secondary fibre elongation is complete when the anterior and posterior ends reach the posterior and anterior poles of the lens and is then considered a mature fibre (Kuwabara, 1975; Kuszak *et al.*, 1988). At the poles, both anterior and posterior ends overlap with other fibres, resulting in regions of optical disorder called sutures (Kuszak *et al.*, 2004b). The epithelial cells go through mitotic divisions and secondary fibres cells elongate throughout life (Kuszak *et al.*, 2004b).

The lens can be thought of as an onion because it is constructed of concentric layers. Each layer is better known as a shell. Given that the lens is continually growing throughout life, the size of the lens and the number of lens fibres increases throughout life (Kuszak *et al.*, 2004b). Each shell has one more fibre than the previous shell. It is known that after the age of five, five new shells are added each year (Kuszak *et al.*, 1996, Oyster, 1999). The fetal nucleus is the layer surrounding the embryonic nucleus. It consists of secondary lens fibres cells and represents the lens at birth. The adult nucleus is the next layer which lies underneath the cortex which sits just under the capsule. The cortex is the outer most part of the lens and it is made up of the youngest fibre cells. Lens cells are permanent, and once

they have differentiated into lens fibres, they can no longer proliferate and drop out of the cell cycle. It is known that lens fibres are relatively the same size between most species, however, it is the number of fibres that accounts for the difference in size of lenses among species (Kuszak *et al.*, 2004a).

2.1.3 Lens sutures

Because fibre shells are continually added throughout life, sutures will continue to grow in depth, extending from the nucleus to the lens poles (Kuszak *et al.*, 2004b, Rao and Maddala, 2006). Suture patterns vary among animals. Sutures are either unbranched or branched and are further classified into umbilical, line, Y or star sutures. The umbilical suture, also called a point suture, is formed when secondary lens fibres meet at a single point and are the only unbranched suture. They are found in avian and reptile lenses (Kuszak *et al.*, 2004b). Branched sutures are found in lenses of all other animals. The line suture is the simplest of branched sutures and it is found in rabbit, frog and most fish lenses (Kuszak *et al.*, 2004a). For lenses containing line sutures, only a few fibres land directly on the anterior and posterior poles; the majority of secondary lens fibres curve away from the poles and land away from the polar axis (Kuszak *et al.*, 2004b). Animals with line sutures have a vertical line at the anterior and a horizontal line on the posterior (Kuszak *et al.*, 1994). The Y suture is the other branched suture and it is the most commonly found type of suture. It is found in mice, dogs and cows. The orientation of the Y suture is similar to that of the line suture; it is upright on the anterior side and inverted on the posterior side (Kuszak *et al.*, 1994). Y sutures are similar to line sutures except they contain an additional branch. Monkeys and humans form the most complex sutures; their sutures are referred to as a “star” suture which

originally arises from a Y suture (Chepelinsky, 2009). Increased branching results in a star shape.

2.1.4 Proteins found within the lens

Proteins account for ninety percent of lens composition (Bloemendal, 1977). The proteins can be broken down into insoluble and soluble proteins. Lens proteins are some of the oldest proteins in the body (Mathias *et al.*, 1997). It is known that different refractive indices exist at different layers of the lens. The crystallin concentration increases from the surface to the nucleus, where the highest refractive index is found (Magid *et al.*, 1992). This gradient of protein concentration corrects spherical aberration, leading to improved lens function (Mathias *et al.*, 1997). Insoluble proteins include cytoskeletal proteins such as microtubules, myosin and actin. Soluble proteins are the α-, β-, γ- and δ-crystallins. Crystallins are recognized for their contribution in light refraction (Lovicu and Robinson, 2004). In chickens, it is known that δ-crystallins are the first crystallins present and are found at the basal region of the lens placode (Zwaan and Ikeda, 1968). In epithelial and fibre cells of the lens in embryonic chicks, δ-crystallins arise first, followed by β-crystallins then finally by α-crystallins (Ikeda and Zwaan, 1967, Rabaey, 1965). The concentration of δ-crystallins is slightly higher in the lens fibre cells compared to the epithelial cell in embryonic lens (Piatigorsky, 1981). In the developing lens, the type of crystallin and their order of appearance differ among species.

In mammals, the first crystallins to appear are the α-crystallins in the lens placode during the invagination of the lens ectoderm (Rabaey, 1965, van de Kamp and Zwann, 1973). Unlike the avian lens, a difference in protein composition is observed in the embryonic lens of mammals, with α-crystallins restricted to the epithelial cells (McAvoy, 1978b). In the

fibre cells of the embryonic lens, α-crystallins appear first, and then the β- and γ-crystallins are expressed. All three crystallins have similar concentrations within the fibre cells (Piatigorsky, 1981). While it is well-known that α-crystallins are the first to appear, the appearance of the where the γ-crystallins is expressed is controversial. In 1970, Shubert *et al.* found that γ-crystallins appeared first in the primary fibres and later in epithelial cells. McAvoy *et al.* disagreed, when they found that γ-crystallins appeared only in the fibre cells (McAvoy, 1978a). Differences in results are likely attributable to differences in the purity of the primary anti-body used.

In amphibians, the first crystallins to emerge are β-crystallins in the primary lens fibre cells of the lens vesicle (McDevitt *et al.*, 1969). In the embryonic lens, the epithelial cells contain a low concentration of β-crystallins only (Piatigorsky, 1981). The fibre cells of the embryonic lens express β-crystallins, followed by the expression of γ- and then α-crystallins. The highest amount of protein within the embryonic nucleus is in the fibre cells and is mainly composed of γ-crystallins with equal concentrations of α- and β-crystallins (Piatigorsky, 1981).

The difference in crystallins synthesis could be due to the differences in the visual system needs or it could be possible that the crystallins share properties that allow them to be used interchangeably (Piatigorsky, 1981). Either way, crystallins are important for the transparency of the lens. The lens must be dense in order to refract light in the aqueous media it is surrounded by (aqueous humor anteriorly and vitreous chamber posteriorly) (Lovicu and Robinson, 2004). It is known that crystallins accumulate to concentrations of 450 mg/mL or greater in the lens fiber cytoplasm (Fagerholm *et al.*, 1981). The solubility of the crystallins, as well as their compact globular structure, is what contributes to their

uniform distribution in the lens cell cytoplasm (Bloemendal *et al.*, 2004). The crystallins are densely packed together to obtain an orderly array within the spaces smaller than the wavelength of light (Mathias and Rae, 1985). As the lens ages, proteins change, with soluble proteins becoming insoluble (Mach, 1963; Hoenders and Bloemendal, 1983).

2.1.5 Metabolism

The lens has its own internal transport system that is composed of ions, pumps and channels. Since the lens is an avascular organ, the transport system is designed to deliver nutrients and remove waste (Mathias and Rae, 1985). The transport system within the lens is critical for sustaining a steady-state cellular volume, as well as maintaining its specialized architecture (Donaldson *et al.*, 2001). The lens is freely permeable to water ions and to other small molecules. Through a network of channels, low resistance gap junctions help maintain a uniform voltage throughout the lens (Mathias and Rae, 2004). As previously mentioned, the lens is a living organ that is continually growing, with older fibres, deep within the nucleus and newer fibres, located in the cortex of the lens. The continual growth results in fibre cells that are at different stages of elongation; this creates variation in the membrane transport system throughout the lens (Mathias and Rae, 2004).

At the surface, the lens is permeable to both Na^+ and K^+ (Brown and Bron, 1996). It is known that the epithelium and newly differentiated fibre cells have Na^+-K^+ pumps and K^+ channels (Donaldson *et al.*, 2001). Mature fibre cells are not as equipped; instead they have a unique mechanism which helps maintain a resting voltage and a constant volume (Mathias *et al.*, 1997). Fibres within the lens communicate by the interconnected gap junctions, which deliver an ionic current (Donaldson *et al.*, 2001). The ionic current is primarily created by

the movement of Na^+ ions. The current enters at the poles, and then along the extracellular clefts between fibre cells. The current then crosses the fibre cell membrane and into the fibre cells (Donaldson *et al.*, 2001). It is thought that that majority of lens Na^+-K^+-ATPase activity is located in the anterior epithelium and at the equator from the lens (Mathias *et al.*, 1997). There are more Na^+-K^+-ATPase pumps located at the equator than the anterior epithelium which corresponds to the flow of current i.e. current enters at the poles and exists at the equator (Gao *et al.*, 2000). The current draws the movement of other ions and molecules through the movement of fluids.

It is known that water brings nutrients to the fibre cells deep within the lens. Water follows Na^+. Water permeability is greatest in the epithelial cells compared to the fibre cells (Donaldson *et al.*, 2001). Aquaporin-0, better known as AQP0, is a major intrinsic protein that is specifically expressed in the lens fibre cells. While aquaporin-0 is best known for its role as a water channel within the lens, it may be important for maintaining lens transparency and accommodation (Chepelinsky, 2009). Mutations associated with AQP0 expression were proven to interfere with interdigitation formation within the lens. It is known that interdigitations are important in keeping the lens transparent because they minimize extracellular space, which reduces large-particle scatter (Al-Ghoul *et al.*, 2003). Proper arrangements of interdigitations are also thought to be important in maintaining the relative positions of fibres during accommodation (Al-Ghoul *et al.*, 2003).

The lens uses glucose as its metabolic fuel for growth and homeostasis (Donaldson *et al.*, 2001). Glucose gets incorporated by specific proteins transporters; GLUT1 is the primary transporter in the lens epithelium and GLUT3 transporters within the cortex of the lens supply glucose to the mature fibre cells (Merriman-Smith *et al.*, 1999). Glucose

metabolism decreases towards the centre of the lens because there are less glucose transporters present in the nucleus than the cortex (Donaldson *et al.*, 2001).

The movement of Cl^- are important for regulating volume changes within the lens (Donaldson *et al.*, 2001). It is thought that Cl^- moves from the extracellular space inwardly to the cytoplasm of mature fibre cell, then back into the extracellular space nearer to the lens surface. With this idea, research has been conducted and used to explain diabetic cataracts. It is known that an increased concentration of glucose leads to a buildup of the intracellular osmolyte sorbitol within the fibre cells (Donaldson *et al.*, 2001). Sorbitol is known to make the Cl^- channels open and induces movement of osmolytes and water into the lens. Peripheral fibres have membrane voltages favouring a Cl^- efflux which causes volume decrease and a return to a normal appearance (Lewis and Donaldson, 1990). However, the deeper, more mature fibres of the lens, favour an influx and this increases the rate of swelling, resulting in cataract formation (Donaldson *et al.*, 2001).

Calcium is an additional ion found at low levels in a healthy lens. The aqueous humour has about six times the amount of calcium compared to the lens (Hightower *et al.*, 1980). The epithelial cells of the lens are in contact with the aqueous humour and therefore, the anterior portion of the lens must regulate the Ca^{2+} levels (Rafferty *et al.*, 1994). Calcium levels are maintained by Ca^{2+}-ATPase pumps, calcium-binding proteins and sodium-calcium exchanges (Brown and Bron, 1996). As the lens ages, permeability to calcium increases. One reason for the increase is because Ca^{2+}-ATPase activity decreases by 50% (Paterson *et al.*, 1997). There are a few other Ca^{2+}-ATPase pumps within the lens and these include Mg^{+}-Ca^{2+}-ATPase and calpain Ca^{2+}-ATPase. Ca^{2+}-ATPase pumps are also affected by temperature. An experiment with calcium and temperature showed that when the

temperature decreased to 4^{o}C, the calcium concentration decreased by 85% compared to the amount of calcium at 37^{o}C (Hightower *et al.*, 1980).

2.2 The Nature of Contractile Microfilaments

2.2.1 Actin and myosin

Actin and myosin are two important components of a contractile system. Non-muscle actin and myosin is referred to as cytoplasmic filaments and they share the same characteristics as muscle tissue (Pollard and Weihing, 1974). It is known that actin is present whenever structural and mobile function is required in eukaryotic cells (Bhadriraju *et al.*, 2007). In all three of the muscle tissue types, actin and myosin interact together to induce a contraction. The power stroke is the basis of contraction. A force is created by a reversible interaction between actin and myosin binding (Pollard and Weihing, 1974). It is generated by the sliding interaction of actin and myosin filaments, with the energy provided by the hydrolysis of adenosine triphosphate (ATP) (Pollard and Weihing, 1974). This concept is known as the sliding filament theory of muscle contraction.

The interaction and contraction is not limited to muscle tissue. The relationship between non-muscle actin and myosin is similar to that of smooth muscle contraction. However, non-muscle myosin appears to be more sparse compared to non-muscle actin. In muscle tissue there is about 500 molecules of myosin and in non-muscle tissue only 10-20 are present (Bhadriraju *et al.*, 2007).

Actin can be found in two forms, either as a monomer globular (g-actin) or as a polymer filamentous (f-actin). The molecular weight of g-actin is between 43-48 kDa (Silverthorn, 2004). It is essential for g-actin to polymerize because only f-actin is capable of

activating myosin ATPase (Korn, 1978). ATPase is needed to hydrolyze ATP into adenosine diphosphate (ADP) and inorganic phosphate (Pi) which is required for contraction (Pollard and Weihing, 1974).

Myosin is a thick filament. Myosin II is the found in muscle tissue as well as in non-muscle tissue such as the lens. It is made up of two heavy chains weighing approximately 200 kDa and two pairs of light chains, weighing between 16-20 kDa (Silverthorn, 2004). The two heavy chains form two globular heads and a rodlike tail, which is a single alpha-helical coiled-coil. Two light chains house the actin-binding site as well as the ATP binding site. The ATP binding domains are the site of ATP hydrolysis. ATP hydrolysis is regulated differently in skeletal and smooth muscle tissue (Pollard and Weihing, 1974).

2.2.2 Muscle contraction

At rest, myosin is in contact with actin at one of many binding sites located along the monomer. When ATP becomes available, it binds to the myosin head, which changes the attraction of the actin-myosin connection. This causes myosin to release the actin to which it is currently attached to. Soon after, the ATP molecule is hydrolyzed to form ADP and Pi. The conversion of ATP to ADP creates energy that is used by the myosin head to swing and bind weakly to a new location on the actin molecule, creating a buildup of potential energy (Silverthorn, 2004). As soon as the Pi is released from the myosin head, the power stroke has been initiated. At that point, the ADP is still attached to the myosin head. Once the ADP is released, the myosin attaches lightly to another location on the actin molecule. At this point the contractile system is ready for the cycle to start again.

Myosin is considered to be an actin-binding enzyme which, together with actin

filaments, creates a contractile system. It is understood that when myosin is colocalised with actin, there is a good chance that a contractile system is present.

2.2.3 Skeletal muscle contraction (voluntary)

A sarcomere is the basic unit of a contractile apparatus in skeletal muscle. Muscle contraction results from the shortening of its sarcomeres. Sarcomeres are found in repeating parallel units, which is what gives the appearance of striations within striated muscle tissue. In skeletal muscle, actin is controlled by two regulatory proteins, tropomyosin and troponin. Tropomyosin is an alpha-helical coiled-coil protein that wraps around the actin filament and partially blocks the myosin binding site (Pollard and Weihing, 1974). Troponin is a calcium dependent protein that controls the position of tropomyosin (Pollard and Weihing, 1974). It is composed of three subunits; 1) troponin-I which is the inhibitory component, 2) troponin-C the Ca^{2+} binding component and 3) troponin-T the subunit that binds to tropomyosin (Pollard and Weihing, 1974). Troponin is situated at intervals of 40 nm along the actin filament and binds to tropomyosin (Spudich *et al.*, 1972). When calcium is present, it binds to the troponin-C component, pulling the tropomyosin away from the myosin-binding site. This frees ups the myosin binding site and allows myosin to bind. When calcium is present in low concentrations, calcium no longer binds to the troponin-C site and tropomyosin shifts to blocking position (Silverthorn, 2004).

2.2.4 Cardiac muscle contraction (involuntary)

Cardiac muscle is a specialized tissue that is only located within the heart. Cardiac muscle fibres are electrically linked to one another with gap junctions that are contained in specialized cell junctions known as intercalated disks (Silverthorn, 2004).

Cardiac muscle is also composed of sarcomeres, which gives the muscle its striated appearance. Cardiac muscle is mediated by the autonomic nervous system (parasympathetic nervous system) while skeletal muscle is innervated by the (voluntary) motor neurons. It should be noted that, like cardiac muscle, the ciliary muscle in chickens show skeletal muscle properties (striations) but are innervated by the autonomic nervous system.

2.2.5 Smooth muscle contraction (involuntary)

Smooth muscle tissue differs from skeletal and cardiac in their structural elements and the contraction process. It is known that smooth muscles have longer actin and myosin filaments. Smooth muscle contractile filaments are not arranged in sarcomeres; instead they are arranged in long bundles that that extend diagonally (Silverthorn, 2004). Smooth muscle cells become globular when contracted. The actin filaments attach to dense bodies within the cytoplasm and myosin bundles lie between the actin filaments and end at the cell membrane on protein attachment plaques (Pollard and Weihing, 1974). Smooth muscle contraction starts with an increase in Ca^{2+}, which is released from the sarcoplasmic reticulum or from the extracellular fluid. Calcium then binds to calmodulin, which activates MLCK. MLCK phosphorylates the myosin light chain (MLC) found on the myosin head, which increases ATPase activity. Contraction results from actin and myosin interactions. Smooth muscle relaxation happens when the events occur in reverse order.

2.2.6 Actin and myosin distributions within the lens

Filamentous actin is located within the lens. A number of studies have been carried out to determine whether a contractile system exists on the lens. In 1978, Rafferty and Goossens studied the cytoplasmic filaments within the lens in variety of species using

electron microscopy. They identified two distinct arrangements of the cytoplasmic filaments. The first arrangement was observed in spherical non-accommodating lenses of mice and rats. These lenses showed sparsely distinctive cytoplasmic filamentous in epithelial cells. They found 1) fibres along the axes of cytoplasmic processes of plasma membranes, 2) a perinuclear bundles of parallel-oriented filaments and 3) subcortical filaments throughout the cytoplasm except for the area bordering the plasma membrane (Rafferty and Goossens, 1978). The second distinct arrangement was observed in accommodating lenses of squirrels and human infants. Unlike the non-accommodating group, no perinuclear sheath or subcortical bundles were observed and few cytoplasmic processes were noted. A three-dimensional lattice of actin fibres was located around the epithelial-lens fibre junctions. These findings correlate with the accommodative ability of the species (Table 1).

In 1984, Rafferty and Scholz further investigated the arrangement of cytoskeletal proteins and their possible functions within the lens. They used transmission electron microscopy on rabbits to study the organization of actin in epithelial cells that cover the anterior surface as well as the fibre cells. The apex of each epithelial cell was covered with polygonal arrays (Rafferty and Scholz, 1984). Specifically, filaments were joined together at a central vertex that extended to central vertices of other cells nearby. They concluded that the polygonal arrays are permanent structures (Rafferty and Scholz, 1984).

In 1985, Rafferty and Scholz investigated the actin arrangements in the rabbit lenses as well as in non-accommodating species the mouse. Again, rabbit lenses were shown to have polygonal arrays consisting of central vertices and interconnecting actin filaments present on the apical ends of the epithelium tissues (Rafferty and Scholz, 1985). Instead of polygonal arrays of actin, mouse lenses exhibited small packets of actin in single, elongated,

curved bundles, which were referred to as "sequestered actin bundles" (Rafferty and Scholz, 1985).

Rafferty and Scholz (1989) did a comparative study on the cytoplasmic proteins of different species and their mechanisms of accommodation. It was observed that animals that accommodate by distorting the anterior surface of the lens, which include squirrels, chipmunks, rabbits, monkeys and humans, all showed polygonal arrays. Animals that accommodate by translating the entire lens, include sharks and bony fish, showed actin structures in a pattern known as "stress fibres" (Rafferty and Scholz, 1989). Animals that accommodate by squeezing the lens, such as, chickens and turtles, showed no specialized actin pattern at the anterior pole.

Rafferty *et al.* identified myosin to be present inside some, but not all, polygonal arrays of actin (Rafferty *et al.*, 1990). From their findings, they speculated that the contractile proteins found on the lens could only contract as a whole sheet (Rafferty *et al.*, 1990). More recently, Bassnett *et al.* did a similar study of the actin-myosin arrangement within the chicken lens. Using confocal microscopy, they found the same arrangement of colocalised actin-myosin on the posterior capsule of the chicken lens (Bassnett *et al.*, 1999).

2.3 Functional Properties of the Lens

2.3.1 Accommodative apparatus

The lens is surrounded by fluid, the anterior part is in contact with the aqueous humour and the posterior part is in contact with the vitreous humour (Chepelinsky, 2009). Suspensory ligaments also known as zonules, attach to the proximal ends of the lens and the distal ends of the ciliary muscle (Walls, 1963). The ciliary muscle is located all around the

lens and is housed in the ciliary body. The lens contents are surrounded by the lens capsule which is elastic in nature (Krag and Andreassen, 2003). The short ciliary nerve controls the contraction of the ciliary muscle (Oyster, 1999).

2.3.2 Theories of accommodation

The most widely accepted theory on the process of accommodation is by Herman Ludwig Ferdinand von Helmholtz (Remington, 2005). In his theory of accommodation, it is believed that an impulse from the oculomotor nerve causes a contraction in the ciliary muscles, making it move inward and forward which relaxes the pull of the zonules (Helmholtz and Southall, 1962). The relaxation of the zonules results in a decrease in the diameter of the ciliary rings surrounding the lens which allows the lens capsule into its preferred spherical shape, resulting in a higher refractive power (Helmholtz and Southall, 1962).

2.3.3 Mechanisms of accommodation in different species

Indirect accommodation occurs by releasing the tension on the zonules and allowing the lens into its preferred thickened shape. Translational accommodation occurs by the movement of a spherically shaped lens within the globe (Fernald and Wright, 1985). The lens moves approximately parallel to the plane of the pupil. Direct accommodation occurs by squeezing the lens into its accommodative state (Table 1).

Table 1: **Mechanisms of accommodation in different species and their corresponding accommodative range.**

Type of Accommodation	Animals	Accommodative Range
Highly Indirect deforming of the lens	human (4 months) human (adolescent) human (60 -70yr) rhesus monkey	20D 14D 1.6 – 1.7D > 30D
Moderate Indirect deforming of the lens	squirrel rabbit	1 – 1.5D 2.5D
Translation	frog fish	4 – 5D 5D
Direct deforming of the lens	chick diving duck non-diving duck turtle	15–17D 70 – 80D 6D > 35D
Little or no accommodation	dog pig cow rat mouse	Minimal Minimal Minimal None None
Sources: Bito *et al.*, 1987; Sivak *et al.*, 1985; Rafferty and Goossens, 1978; Ott, 2006; Henze *et al.*, 2004; Kuszak *et al.*, 2006; Schaeffel *et al.*, 1999; Glasser *et al.*, 1995; Tsonis, 2008		

2.3.4 Human versus chicken accommodation

Chickens and humans both deform the lens in order to achieve accommodation. Chickens are precocial; they open and use their eyes the day of hatching the same way humans do. Chickens are diurnal species that sleep when it is dark and active in bright

conditions. Anatomically, chicken eyes are similar because the postganglionic ciliary nerve innervates the ciliary muscles in both (Dryer, 1994). However, there are a few differences in the chicken eye compared to a human eye. One major distinction lies in the structure of the ciliary muscle. The human ciliary muscle is classified a smooth muscle while the avian ciliary muscle is striated and structurally similar to skeletal muscle. However, both are innervated by the autonomic nervous system (Murphy *et al.*, 1995)

Accommodation in a chicken occurs very differently from that in humans. Avian ciliary muscle contraction results in direct squeezing of the lens, whereas in humans ciliary muscle, contraction releases the tension of the zonules, which are holding the lens in an accommodative state (Sivak, 2008). Direct manipulation of the avian lens is possible because of its structural adaptations. These adaptations include, 1) enlarged ciliary folds which allow for direct contact with the lens, 2) Scleral ossicles, which provide a greater range of movement for the lens and 3) annular pads which increase the diameter of the lens (Willekens and Vrensen, 1985, Sivak *et al.*, 1986).

2.4 Lens Disorders

2.4.1 Presbyopia

Presbyopia is a condition related to the aging lens. It is the progressive reduction in accommodation. The underlying cause of presbyopia is unclear. However, there are number of theories as to why people develop presbyopia which can be divided into two categories, lenticular or extra-lenticular (Charman, 2008). Lenticular includes the lens and its capsule, whereas extra-lenticular includes the support structures around the lens.

Duane's theory states that presbyopia results from ciliary muscle degeneration (Pierscionek, 1993) which leads to the the progressive weakening of the ciliary muscle, and ultimately a reduction in accommodative ability (Duane, 1925). Similar to the Duane theory is the Helmholtz-Hess-Gullstrand theory, which focuses on the biomechanical changes; it is based on the fact that the lens is continually increasing in mass as new fibres are being added as a result of aging. This progressive increase in bulk mass results in the lens becoming less pliable (Oyster, 1999). There is an increase in weight from 66 mg at birth to approximately 264 mg at age seventy five, which further supports this idea of the lens continually growing, causing it to become mechanically less responsive (Scammon and Hesdorffer, 1937).

2.4.2 Cataracts

A cataract is an opacity in the lens that absorbs and scatters light, rather than allowing the light to travel right through. Cataracts reduce visual acuity because they prevent light from entering the eye, which is needed to allow the refracted light to hit the retina (Oyster, 1999). Cataracts can occur at all ages but the majority of cases appear after the age of fifty. They are easily classified by the location of where they are formed within the lens. They can occur at the cortex, nucleus and anterior/posterior capsule. Their names correspond to their location; cortical, nuclear, and anterior/posterior subcapsular cataracts. People with cortical cataracts have opacities in the outer lens shells. Nuclear cataracts first appear in the centre of the lens and may grow outward to encompass the cortex (Vrensen, 2009). The third and least common type of cataracts is the anterior/posterior subcapsular cataracts. These cataracts have opacities that lie in the outer layer of the cortex at the anterior and posterior poles. The most prevalent type of cataract is age-related and is named senile cataracts, which mainly

occur in the cortex. Cataract can appear from other reasons besides aging. Some cataracts may form after eye surgery, such as vitrectomy or they can result from other health problems such as diabetes. People can also get cataracts from eye injuries or radiation exposure. Cataracts can also be congenital. The exact cause of cataract formation is still unclear, however, there are a few theories that are becoming more accepted. The ones that are most relevant to this thesis include UV exposure and changes in intracellular calcium.

The most widely accepted cause of cataractogenesis is the cumulative effects of exposure to sunlight, in particularly the ultraviolet component. It is known that the ratio of soluble to insoluble proteins changes as people age. Younger lenses have more soluble proteins than older lenses. The increased accumulation of insoluble proteins is directly correlated to the development of nuclear cataracts (Shubert *et al.*, 1970). Older people have a greater cumulative exposure to ultraviolet light from the sun. It is known that absorption of UVB light is hazardous to the eye and causes optical changes and metabolic disturbances (Oriowo, 2003). This continued absorption of high-energy photons breaks chemical bonds both directly and indirectly (Oyster, 1999). Breaking the bonds results in increased heat by reradiation as well as increased rates of oxidation. Both processes change the structure of the proteins in the lens, resulting in insoluble aggregates. A decline in lens cellular metabolic activity with no signs of recovery was confirmed after porcine lenses were treated with UVB radiation (Oriowo, 2003).

An increase in intracellular calcium within the lens is also known to cause cataracts. Calpain is a calcium-dependent cysteine protease which cleaves the substrates of the α and β-crystallins (Azuma *et al.*, 1995). This degradation destroys the ordered arrangement of crystallins within the lens and results in opacification (Sanderson *et al.*, 1996). A study by

Azuma *et al.*, found that proteolysis by calpain is an underlying mechanism for sugar-induced cataracts. Aldose reductase is an enzyme that converts glucose into its alcohol form known as sorbitol. By using a reductase inhibitor, osmotic changes were disturbed, preventing the calcium influx needed to activate calpain (Azuma *et al.*, 1995). Their findings demonstrated the relationship between sugar-induced cataracts and calcium.

An increase in cytoplasmic calcium also affects the cytoskeleton of the lens including actin and microtubules (Sanderson *et al.*, 1996). Again, a calcium influx activates calpain which also results in breakdown of microfilaments into multiple small round cells results, a process known as globalization (Bhatnagar *et al.*, 1995). It is thought that globalization is responsible for the light scattering centres (Bhatnagar *et al.*, 1995)

2.5 Objective

The objective of this experiment was to investigate the cytoskeletal proteins found on the lens during avian accommodation. Given the actin-myosin arrangement at the lens surfaces, there are speculations that these contractile proteins could play a significant role in mediating the cellular changes that occur during accommodation. The purpose of this experiment was to inhibit one of the proteins needed for contraction and see if a change in accommodation could be detected.

III. Methods

3.1 Electrophysiological Apparatus

In order to induce accommodation, an electrical pulse was needed to send stimulus through the ciliary nerve. A suction electrode was made. Two pieces of silver wire (AM systems Inc 7825) were sanded down with fine sanding paper to remove oxidized chloride. Wires were observed under a microscope to ensure that the entire wire was completely sanded. Wires were placed in 100% bleach for 20 minutes to coat the wires with chloride ions. Then the wires were then rinsed in deionized water for 10 minutes. Tygon® tubing (S-50-HL-Class VI) was measured and cut to fit a metal rod. A 5 mL syringe (Becton-Dickinson 9605) was attached in one end of the tubing. A plastic connecting piece (Cole-Parmer Instrument Co. 06359-07) was attached in other end. An inch away from the syringe, a small hole with a diameter of 2 mm was cut and one of the silver wires was placed through the tube all the way to the tip of the plastic piece. The other silver wire was evenly wrapped around the entire length of the tubing. The wire within the tube was soldered to the positive (+) stimulation wire and the outer wire was soldered to the negative (–) stimulation wire. Epoxy glue was used to close the hole in the tube as well as to glue the tube to the rod.

Suction electrode tips (Tygon® tubing AAQ02133) were heated gently and then stretched. Under a microscope, tips were cut in order to ensure a tight fit onto the ciliary ganglion and nerve. The unheated end of the suction tip was attached onto the connecting piece. The suction electrode was supported by a micro manipulator. Positive and negative stimulation wires were hooked up to their corresponding slots in the Photo-Optic Stimulation

Isolation Unit (Grass PSIU6), which was connected to an S43 Grass stimulator.

3.2 Experimental Procedures

3.2.1 Dissection and treatments

White leghorn hatchling chicks (*gallus gallus domesticus*) were obtained from Maple Leaf, New Hamburg, Ontario, Canada and were fed *ab libitum*. Lights were on a 14:10 light: dark cycle.

Chicks were sacrificed by decapitation at 6 days. Heads were bisected along the sagittal plane. The ciliary nerve and ganglion for each eye were carefully freed from surrounding tissue and left intact. Eyes were enucleated and extra tissue was removed. The posterior globe was removed, leaving a wedge containing the ciliary nerve and ganglion intact. The sclera was removed as close to the lens as possible without damaging the ciliary muscle so that the lens could be viewed by the cameras. All dissections were carried out in oxygenated (95% oxygen, 5% carbon dioxide) Tyrode's saline (TS: 134mM NaCl, 3 mM KCl, 20.5 mM $NaHCO_3$, 1 mM MgCl, 3 mM $CaCl_2$, in water).

Eyes were submerged in oxygenated Tyrode's saline containing either ML-7 or vehicle for 15 minutes. The ML-7 groups contained the ML-7 powder dissolved in 50% water and 50% ethanol (EtOH) whereas the vehicle groups contained only 50% water and 50% EtOH. The ML-7 dosage groups were 1 μM in 0.001% (v/v) EtOH, 10 μM in 0.01% (v/v) EtOH or 100 μM in 0.1% (v/v) EtOH and the vehicle dosage groups were 0.001% (v/v) EtOH, 0.01% (v/v) EtOH or 0.1% (v/v) EtOH respectively. Eyes were then washed in oxygenated Tyrode's saline (3×10 min). Each wash involved a new tube containing fresh Tyrode's saline. Either the right or left eye of each pair was treated with ML-7 and its fellow

(vehicle) eye was treated with vehicle. Another experiment (no-wash) consisted of the same steps as above except that the (3×10 min) wash step was eliminated.

3.2.2 ML-7

ML-7 is a MLCK inhibitor. MLCK is an enzyme that is Ca^{2+}/calmodulin-dependent and is responsible for catalyzing phosphate from ATP to myosin light chain (MLC) which is needed muscle contraction. ML-7 is expected to disrupt any potential actin-myosin interactions found within tissues containing contractile proteins.

Another MLCK inhibitor is 1-(5-Chloronaphthalene-1-sulfonyl)-1H-hexahydro-1,4-diazepine hydrochloride (ML-9), however, it also inhibits other proteins such as GLUT4 and GLUT1 and it must first be dissolved in 100% ethanol, whereas ML-7 only requires 50% ethanol (Sigma-Aldrich, 2009). Therefore, ML-7 was the inhibitor or choice. It has been successful in studies involving ocular tissue (Rosenthal *et al.*, 2005; Tian *et al.*, 2000)

3.2.3 Measurements of accommodation

The eye was pinned to a Sylgard® washer, cornea facing down. The eye was then placed into a glass chamber that was specially designed to allow access to the ciliary nerve. The chamber with the eye was placed optical laser scanning monitor (Scantox®) (Figure 1). The suction electrode was passed through a small tube and aligned to the ciliary nerve. The rest of the small tube was plugged with petroleum jelly. The chamber was filled with 20% fetal bovine serum in Tyrode's saline to visualize the refracted beams. The ciliary nerve was suctioned into the electrode tip.

The back vertex focal length (BVFL) is the distance from the back vertex of the lens to where a refracted beam crosses the optical axis. BVFL values of ML-7 and vehicle-treated

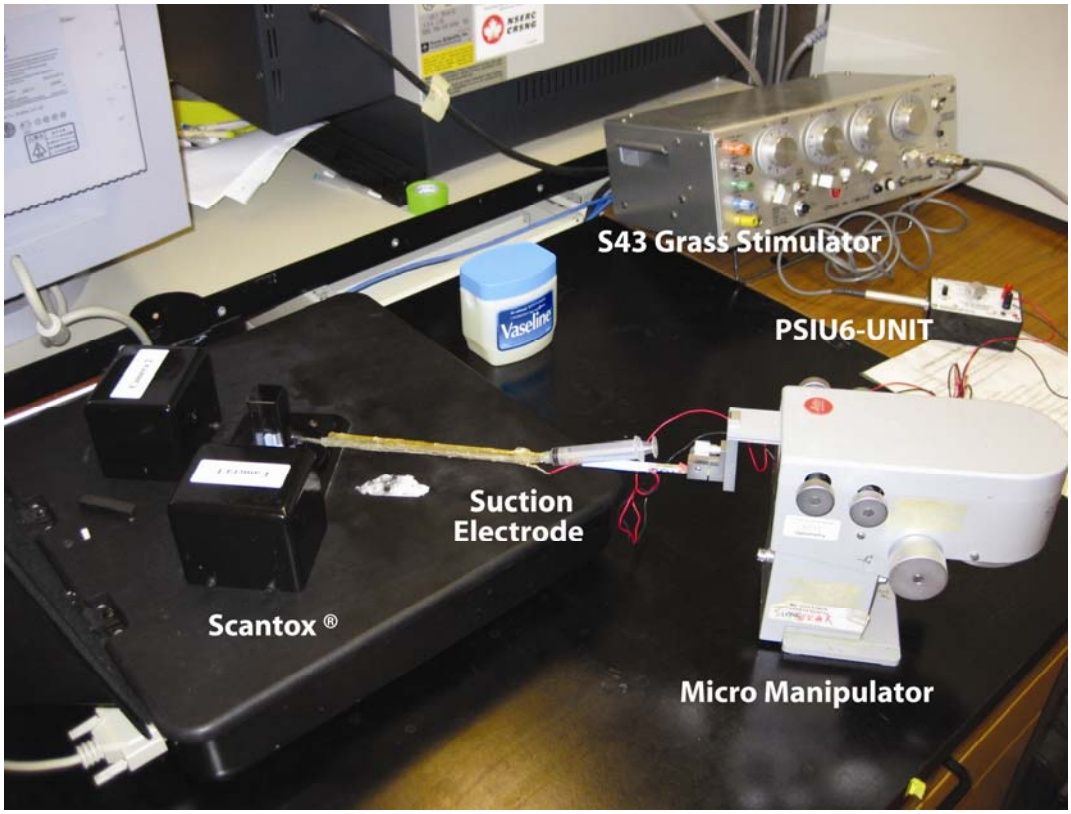

Figure 1: Electrophysiological apparatus

eyes were measured using the Scantox®. The back vertex was determined using a camera image; a low powered helium laser passed through the lens at different eccentricities from the optical axis and refracted beams were captured by two cameras. The Scantox® program was set to capture refracted beams for a diameter of 3.17 mm (slightly larger than the aperture of the pupil at rest) at 0.133 mm intervals. Three scans were obtained; pre-stimulation, stimulation and post-stimulation states. Accommodation of the intact eye was induced by electrical stimulation of the ciliary nerve (30Hz 1-1.5 mA) using the hand made suction electrode.

3.2.4 Detection of phosphorylated myosin by Western blotting

Western blots were used to show the amount of phosphorylated myosin in the presence of ML-7 and without to determine whether ML-7 had an inhibitory effect. A separate set of birds were obtained, maintained and sacrificed as above. Treatment duration and concentrations of ML-7 and vehicle were the same as for the accommodation measurements (Section 2.2.1). Eyes were dissected the same way except for an extra step to remove the posterior capsule. Eyes without the posterior globe were pinned to a Sylgard® dissecting dish with the cornea facing down. Vitreous was completely removed using a probe. A continuous incision was made along the equator of the lens. The posterior capsule was slowly peeled off and stored in 20 µL of Phosphate-Buffered Saline (PBS: 137 mM, NaCl, 3 mM KCl, 101 mM Na_2HPO_4, 2 mM KH_2PO_4, in water) and kept on ice. Capsules were then homogenized in the same buffer. Biostab, a biomolecular storage solution (Biomol; 62513), was added at 20% of the sample volume. Capsule samples were stored in 3 µL aliquots at –80 ºC.

Capsule samples were centrifuged at 3,786 × g for 10 minutes at 4ºC. The supernatant was used for the Western blots. The total protein concentration of each sample was quantified using BioRad DC protein assay™. Eight bovine serum albumin standards were used (125 µg/mL, 250 µg/mL, 500 µg/mL, 750 µg/mL, 1000 µg/mL, 1500 µg/mL, and 2000 µg/mL; Pierce; 23208) with PBS as a control. To determine the absorbance of the standards, 3 µL of each standard were separately placed into a microplate. Then, 3 µL of each capsule sample were placed into the wells adjacent to the standards. A colourimetric change was created by adding 25 µL of reagent A (alkaline copper tartrate) and 200 µL of Reagent B (folin reagent). The plate was tapped gently to mix reagents. After 15 minutes,

the microplate was placed into a Thermo Labsystems Mulitskan spectrum™ spectrophotometer and absorbencies of each well were measured. Capsule samples that showed higher absorbance readings than the highest standard were diluted. Absorbance values were exported into a spreadsheet.

Concentrations of proteins were determined by graphing the absorbance versus amount (in µg) per well of the eight known standards. Using the resulting linear equation $y = mx + b$, the amount of protein per well of capsule samples was calculated. The lowest protein concentration was used to normalize the other samples. Capsule samples were mixed with various amounts of gel loading buffer (GLB: 100 mM Tris base pH 7.4, glycerol 5% (v/v), 2.5% SDS (v/v), bromophenol blue 0.03% (w/v), in water) so that the final volumes were equal. Capsule samples were kept on ice to avoid potential protein degradation. When ready to run, the Western blot capsule samples were heated for 3 minutes at 95ºC.

Proteins were separated with a GE Phastsytem™ and loaded at 1 µL per well on an 8 well comb. For each Western blot, samples were run at the same concentrations to ensure equal loading of protein. Protein concentration varied between blots depending on the lowest concentration of protein for that experiment. Concentrations below 1 µg/µL were not used. Samples were organized so that ML-7- and vehicle-treated eyes of the same bird ran side by side one another. A polyacrylamide PhastGel ™ with a Gradient 10-15 was used (GE Healthcare Bio-Sciences; 57-6781-00). SDS Buffer strips were used to send a current through the proteins (GE Healthcare Bio-Sciences 17-0515-01). The Phastsystem™ ran at 250 V at 15ºC for 30 minutes.

Proteins from the gel were electro-transferred onto wet immuno-blot polyvinylidene-difluoride (PVDF) membranes (BioRad 162-0176). Membranes were wet with methanol and then soaked in 90% transfer buffer (TB: 2.4 g/L Tris, 11.6 g/L glycine, water) and 10% methanol for 30 minutes. The membrane and gel were then placed on three stacked filter papers (Pharmacia Biotech; 18-1003-18) wetted with transfer buffer, with the gel facing up. Three more stacked and wetted filter papers were placed on top of the gel. The transfer was done using the Phastsystem™ PhastTransfer™.

After electro-transfer, membranes were dried at room temperature for 15 minutes; they were placed in an oven at 50ºC for 45 minutes. Membranes were cooled and re-wet in methanol for 1 minute. Methanol was washed off with PBS containing Tween-20 (PBS-T: 05% (v/v) Tween-20 (Sigma Ultra P7949) in PBS) for 5 minutes.

Membranes were blocked in blocking buffer (BB: 8% skim milk powder (w/v) in 0.5% PBS-T) for 45 minutes then washed in PBS-T (5 minutes). Membranes were submerged face-up in anti-phospho-myosin (Sigma M6068, 1:1000 in 90% (v/v) PBS-T and 10% (v/v) BB) on a shaker at 4ºC overnight. Following incubation, membranes were washed (4×5 min) in PBS-T. Anti-phospho-myosin was labeled with horseradish peroxidase-conjugated goat anti-rabbit IgG solution (H & L, abcam ab6721, 1:1000 in 90% (v/v) PBS-T and 10% (v/v) BB; 1 hour, on a shaker at room temperature). Membranes were washed (3×5 min) with PBS-T and then with PBS for 1 minute.

Proteins were visualized with chemiluminescent ECL™ detection (Amersham Biosciences; RPN2132, RPN2133) and imaged using the Storm 840™ imaging system.

3.3 Analysis of Data

3.3.1 Back vertex focal lengths

Back vertex focal lengths (BVFL) of each eye were exported to a spreadsheet. For each scan, the three central points were removed because of the presence of sutures, regions of optical disorder that can over- or under-estimate back focal lengths (Figure 2b). For each pair of eyes, the accommodation scan with the smallest number of beams was the standard for all other scans for that chick. All BVFL values were converted into dioptric values using the refractive index of water, n=1.33. Accommodative amplitude was calculated as the difference between the average of pre-stimulation and the average of post-stimulation (Figure 2c). Interocular differences were calculated by subtracting the accommodative amplitudes of ML-7-treated eyes from the accommodative amplitudes of vehicle-treated eyes.

3.3.2 Detection of phosphorylated myosin

Protein expression was measured by quantifying the amount of fluorescence using the ImageQuant™ software. Vehicle- and ML-7-treated eyes from the same bird were placed side by side on the same gel and were comparisons of the relative amounts of fluorescence were made using the densimetric peak values obtained for each sample.

3.3.3 Statistical analysis

Repeated measures analysis of variance (ANOVA) was used to determine changes in back vertex focal lengths as a function of inhibition treatments (ML-7 versus vehicle), dosage groups (1 μM, 10 μM and 100 μM) and accommodative state (pre-stimulation, stimulation and post-stimulation). Changes associated with accommodative amplitude were also assessed using repeated measures ANOVA as a function of inhibition treatments and dosage

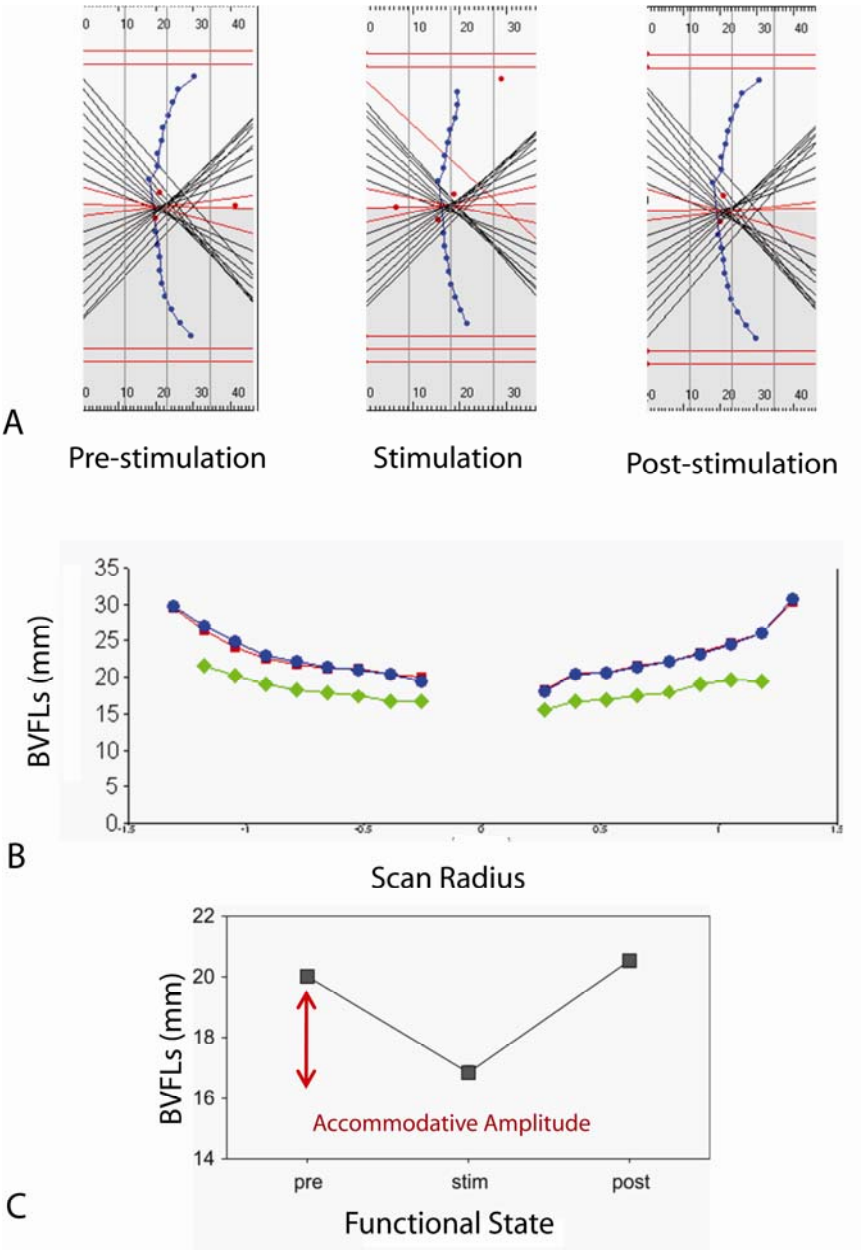

Figure 2: Representative graphs showing data collected from the Scantox®. A: An image taken from the Scantox® for each functional state. B: Line graph showing the three scans. Red: pre-stimulation; Green: stimulation; Blue: post-stimulation Note stimulation scan (green) shows the shortest BVFLs. C: Mean BVFLs of the same scans (not yet converted to dioptric values). The difference between pre-stimulation scan and post-stimulation scan in dioptric values equals the amount of accommodative amplitude.

group. To determine whether washing had an effect on inhibition treatment, a factorial ANOVA was used to analyze the interocular differences in accommodative amplitudes with dosage groups and experiment as factors. A one-way ANOVA was used to analyze the interocular differences in accommodative amplitudes between the wash and no-wash experiment. Greenhouse-Geisser epsilon-adjusted values were used for epsilon values of less than 0.75 where appropriate. Bonferroni-corrected multiple comparison tests were used as the post-hoc test for dependent, repeated data. Results were significant at $p < 0.05$.

IV. Results

4.1 Accommodation Experiments

4.1.1 Experiment 1 (3×10 min) wash

The average number of beams passing through the lens was dependent on the physiological state being measured. In all three dosage groups (1 μM, 10 μM and 100 μM), the stimulation state had fewer beams compared to the relaxed states ($p<0.0001$; Table 2). In the 1 μM group, the pre- and post-stimulation scans had the same average number of beams for the ML-7 and vehicle-treated eyes. However, there was a difference in the stimulation scan; vehicle-treated eyes had an average of one less eccentric point than the ML-7-treated eyes. A similar pattern was observed in the 10 μM group except more beams were obtained for both groups. A different pattern was demonstrated in the 100 μM group; eyes treated with ML-7 had one less eccentric point for all three scans compared to eyes treated with vehicle.

Average back vertex focal lengths for the 1 μM group at the pre-stimulation states were 18.72 ± 0.42 mm (s.e.m) for vehicle-treated eyes and 18.83 ± 0.45 mm eyes and for ML-7-treated eyes (Table 3). During accommodation BVFLs decreased to 15.48 ± 0.63 mm and 16.05 ± 0.78 mm for vehicle- and ML-7-treated eyes, respectively. After accommodation, they jumped back to 18.58 ± 0.29 mm and 18.86 ± 0.47 mm respectively. The 10 μM group had slightly higher BVFLs at the pre-stimulation state for both groups, with an average of 20.18 ±.48 mm for vehicle-treated eyes and 20.28 ± 0.35 mm for ML-7-treated eyes. As expected, shorter BVFLs were measured during the stimulation state with

Table 2: Mean number of beams (± s.e.m) and range entering the pupil for each functional state for lenses treated with vehicle and ML-7 followed by a (3×10 min) wash

Group	Mean ± s.e.m and range in parenthesis of the number of beams entering the pupil for each functional state of accommodation					
	Vehicle Treated Eyes			ML-7 Treated Eyes		
	Pre	Stim	Post	Pre	Stim	Post
1 μM (n=4)	17 ± 0.41 (16-18)	13 ± 0.65 (12-15)	17 ± 0.29 (16-17)	17 ± 1.08 (15-20)	14 ± 0.41 (13-15)	17 ± 0.29 (16-17)
10 μM (n=12)	18 ± 0.43 (16-19)	14 ± 0.51 (12-16)	18 ± 0.57 (14-20)	18 ± 0.29 (15-19)	15 ± 0.43 (12-16)	18 ± 0.38 (15-20)
100 μM (n=4)	18 ± 0.41 (17-19)	15 ± 1.41 (11-17)	18 ± 0.75 (16-19)	17 ± 0.82 (15-19)	14 ± 1.03 (13-16)	17 ± 1.11 (16-20)

Table 3: Back vertex focal length range and mean (± s.e.m) for each functional state for lenses treated with vehicle and ML-7 followed by a (3×10 min) wash

Group	Focal length ranges (mm) and mean focal lengths ± s.e.m (mm) in parenthesis for each functional state of accommodation					
	Vehicle Treated Eyes			ML-7 Treated Eyes		
	Pre	Stim	Post	Pre	Stim	Post
1 μM (n=4)	17.71- 19.51 (18.72 ± 0.42)	14.74- 17.35 (15.48 ± 0.63)	17.86-19.19 (18.58 ± 0.29)	17.79 -19.73 (18.83 ± 0.45)	14.51- 17.40 (16.05 ± 0.78)	17.76-19.68 (18.86 ± 0.47)
10 μM (n=12)	16.34-21.63 (20.18 ±.48)	14.16-19.57 (16.37 ± 0.41)	17.31-22.04 (19.97 ± 0.41)	17.71-22.17 (20.28 ± 0.35)	14.58-19.14 (16.98 ± 0.39)	18.09-21.19 (20.23 ± 0.32)
100 μM (n=4)	19.13-22.17 (21.10 ± 0.68)	16.32-19.24 (17.68 ± 0.61)	18.97-22.10 (21.06 ± 0.73)	17.67-20.90 (20.01 ± 0.78)	14.08-18.78 (16.85 ± 1.08)	17.67-22.28 (20.53 ± 1.00)

values averaging to 16.37 ± 0.41 mm for vehicle-treated eyes and 16.98 ± 0.39 mm for eyes treated with ML-7. Post-stimulation BVFLs increased to 19.97 ± 0.41 and 20.23 ± 0.32 for vehicle- and ML-7-treated eyes, respectively. A change in back vertex focal lengths was not noticed for the 100 μM group compared to the 10 μM group. For vehicle-treated eyes, an

average 21.10 ± 0.68 mm was obtained at the pre-accommodative state, which was slightly higher compared to their fellow of ML-7-treated eyes at 20.01 ± 0.78 mm. During the accommodative state, BVFLs shortened to 17.68 ± 0.61 mm in vehicle-treated eyes and 16.85 ± 1.08 mm for ML-7-treated eyes. BVFLs then increased to 21.06 ± 0.73 mm and 20.53 ± 1.00 mm at the post-accommodative state respectively.

A two way repeated measures ANOVA revealed that for all three dosage groups (1 μM, 10 μM and 100 μM), focal lengths at the stimulation state were shorter than those at rest ($p<0.0001$; Figure 3). This was expected since it is known that the refractive power increases with accommodation resulting in shorter back vertex distances. Similar results were observed in a study by Choh *et. al* (2002). There were no interactions detected between dosage groups and inhibition treatments ($p=0.1693$; Figure 3). Although the results were not significant, the following trend was observed: For eyes at rest (pre- and post-accommodative states), the BVFLs of the ML-7-treated eyes for the 1 μM and 10 μM groups tended to be at the same lengths as vehicle-treated eyes ($p=1.000$ and $p=0.9994$, respectively; Tukey; Figures 3a and 3b). However, the BVFLs of ML-7-treated eyes during the stimulation state for these groups were slightly, although not always significantly, longer compared to vehicle-treated eyes ($p=0.6759$, $p=0.0158$, respectively; Tukey). In contrast, BVFLs of the vehicle-treated eyes in the 100 μM dosage group tended to have longer BVFLs for all three physiological states (pre-stimulation, stimulation, post-stimulation) compared to the ML-7-treated eyes ($p= 0.0103$, $p=0.1232$ and $p=0.7899$, respectively; Tukey; Figure 3c).

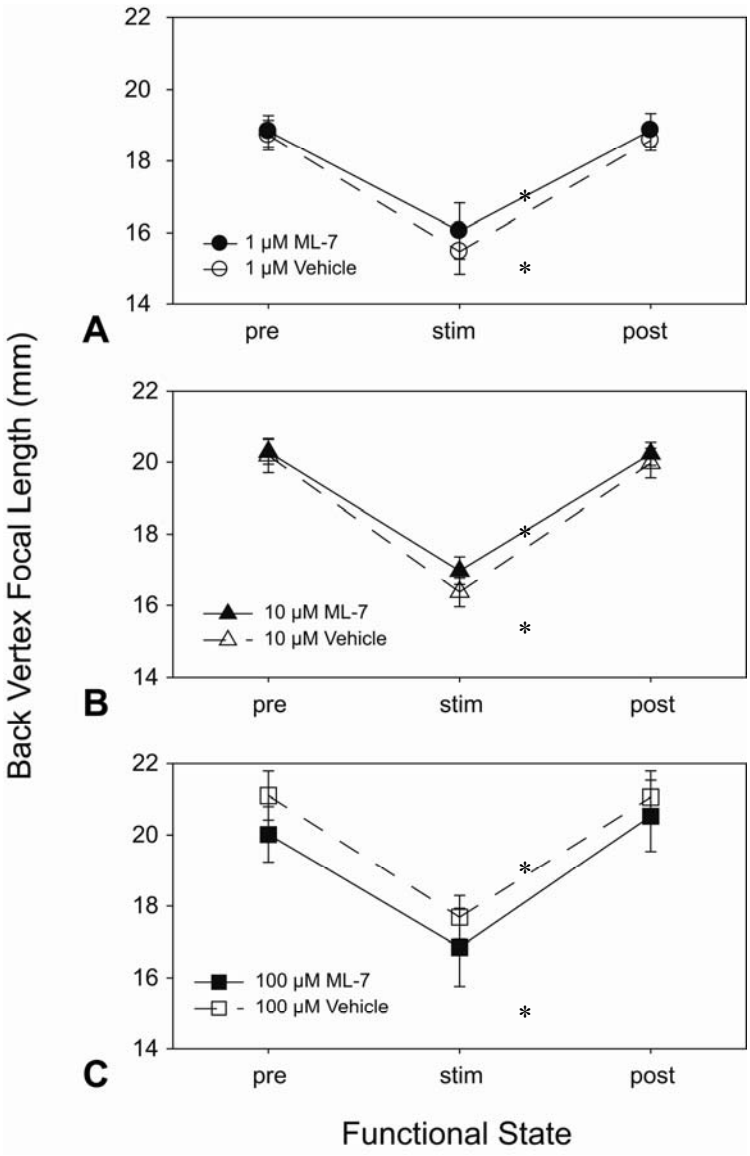

Figure 3: Line graphs showing the mean back vertex focal lengths (± s.e.m) for lenses treated with vehicle and ML-7 with a (3×10 min) wash. A: 1 µM (n=4), B: 10 µM (n=12), C: 100 µM (n=4). For all three groups focal lengths for the stimulation state were significantly shorter that those at rest (P < 0.0001) which are denoted by asterisks.

The amount of accommodation was determined by the difference in BVFLs between the pre-stimulation and stimulation states. All focal lengths were converted into dioptric values and then the pre-stimulated values were subtracted from values measured during stimulation (see methods section 3.3.1). For all three dosage groups, vehicle-treated eyes had higher accommodative amplitudes compared to ML-7-treated eyes. Although no interactions were detected between dosage groups and inhibition treatments (p=0.8076; Figure 4), when dosage groups were collectively gathered, a difference was detected (p=0.0289; Figure 4).

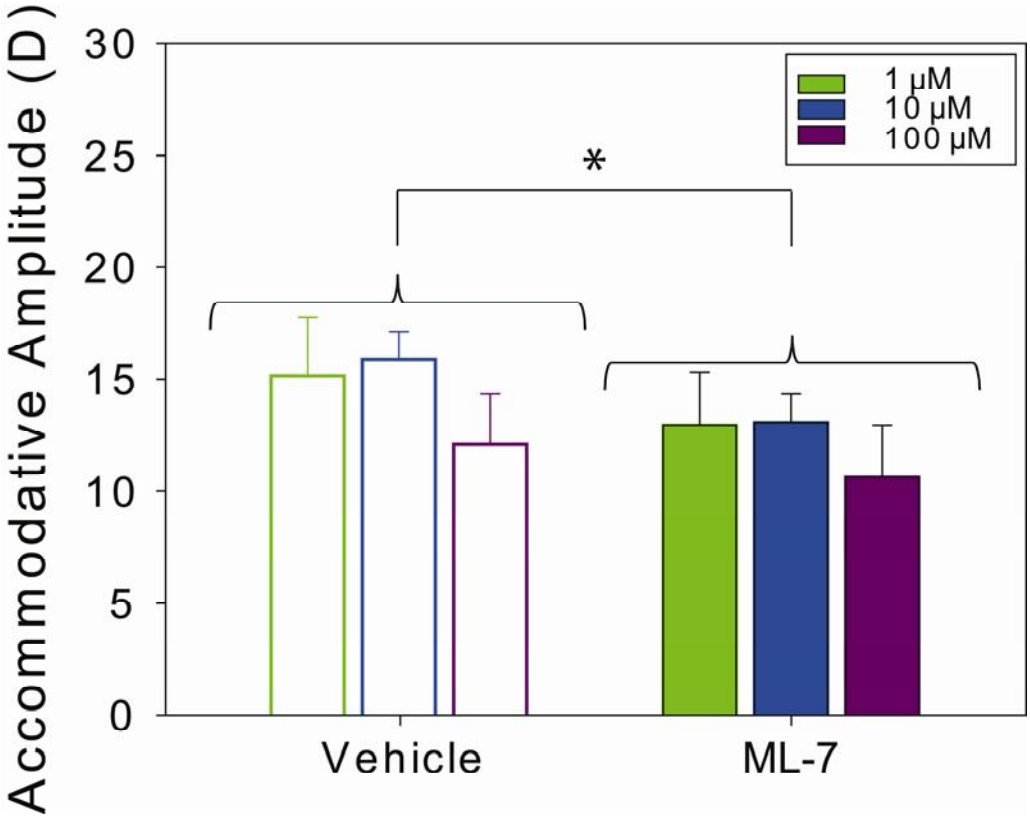

Figure 4: Bar graph showing mean accommodative amplitudes (± s.e.m) of vehicle- and ML-7-treated eyes with a (3×10 min) wash for all three dosage groups 1 µM (n=4), 10 µM (n=12) and 100 µM (n=4). When grouped by inhibition treatment (vehicle and ML-7), accommodative amplitudes for ML-7 treated eyes were significantly lower than vehicle-treated eyes (p=0.0289) which is denoted by an asterisks.

Eyes treated with ML-7 had significantly shorter accommodative amplitudes compared to vehicle-treated eyes.

4.1.2 Experiment 2 no-wash

As with the wash experiment, the average number of beams passing through the lens was different depending on the physiological state. In all three dosage groups, there were fewer beams obtained in the stimulation state compared to the pre-stimulation and post-stimulation states ($p<0.0001$; Table 4). In the 1 μM group, there was an average of one less

Table 4: Mean number of beams (± s.e.m) and range entering the pupil for each functional state for lenses treated with vehicle and ML-7 without a wash.

Group	Mean ± s.e.m and range in parenthesis of the number of beams entering the pupil for each functional state of accommodation					
	Vehicle Treated Eyes			ML-7 Treated Eyes		
	Pre	Stim	Post	Pre	Stim	Post
1 μM (n=4)	17 ± 0.55 (16-19)	13 ± 0.73 (11-15)	17 ± 0.80 (14-19)	17 ± 0.40 (16-18)	14 ± 0.37 (13-15)	18 ± 0.20 (17-18)
10 μM (n=12)	18 ± 0.19 (17-19)	14 ± 0.33 (11-16)	17 ± 0.18 (16-18)	17 ± 0.28 (16-19)	14 ± 0.48 (10-15)	17 ± 0.31 (15-19)
100 μM (n=9)	16 ± 0.65 (12-18)	14 ± 0.56 (11-16)	17 ± 0.46 (15-19)	17 ± 0.49 (15-19)	13 ± 0.39 (11-15)	17 ± 0.33 (16-19)

eccentric point for the stimulation state in the vehicle-treated group compared to the ML-7-treated group. The average of number of beams entering the pupil for the post-stimulation scan in the 1 μM ML-7 group was one more than those of the pre-stimulation state within its own group and of the post-stimulation state with the vehicle-treated group. Vehicle-treated eyes in pre-stimulation state of the 10 μM group had an average of one more beam than that of the pre-stimulation state ML-7-treated eyes. For the stimulation and post-stimulation

states, ML-7- and vehicle-treated eyes shared the same average number of beams entering the pupil. Vehicle-treated eyes for the 100 μM group had one less eccentric point at the pre-stimulation state and one more for the stimulation state compared to the ML-7-treated eyes.

Again, for all three dosage groups, two way repeated measures ANOVA revealed that focal lengths at the accommodative state were shorter than those at rest ($p<0.0001$; Figure 5). Interactions were detected between dosage group and inhibition treatments ($p=0.0053$; Figure 5), however, after Bonferroni multiple comparison testing, no differences were detected. Average BVFLs for the 1 μM group at the pre-stimulation state for vehicle-treated eyes were 21.10 ± 0.68 mm and 20.01 ± 0.78 mm for the ML-7-treated eyes (Table 5). During the accommodation state, they lowered to 17.68 ± 0.61 mm and 16.85 ± 1.08 mm, respectively. At the post-stimulation state, focal lengths went back up to 21.06 ± 0.73 mm for vehicle-treated eyes and for 20.53 ± 1.00 ML-7-treated eyes. The 10 μM and 100 μM groups had slightly lower average focal lengths for each physiological state compared the 1 μM group (Table 5). The ML-7-treated eyes for the 10 μM group had an average BVFL of 20.16 ± 0.48 mm during the pre-stimulation state, which was slightly lower compared to their fellow vehicle-treated eyes, which averaged to 19.36 ± 0.44 mm. At the accommodative state, BVFLs shortened to 15.34 ± 0.37mm and 15.76 ± 0.39 mm for vehicle- and ML-7-treated eyes, respectively; they then increased to 19.16 ± 0.39 mm and 20.04 ± 0.45 mm, respectively, during the post-accommodative state. ML-7-treated eyes in the 100 μM group had slightly higher BVFLs at the pre-stimulation state compared to vehicle-treated eyes at the same state at 19.62 ± 0.6 mm (ML-7) and 19.12 ± 0.54 mm (vehicle-treated eyes). As expected, shorter BVFLs were measured during the stimulation state, with values averaging to 15.37 ± 0.51 mm for the ML-7 group and 15.00 ± 0.48 mm for the vehicle group. The

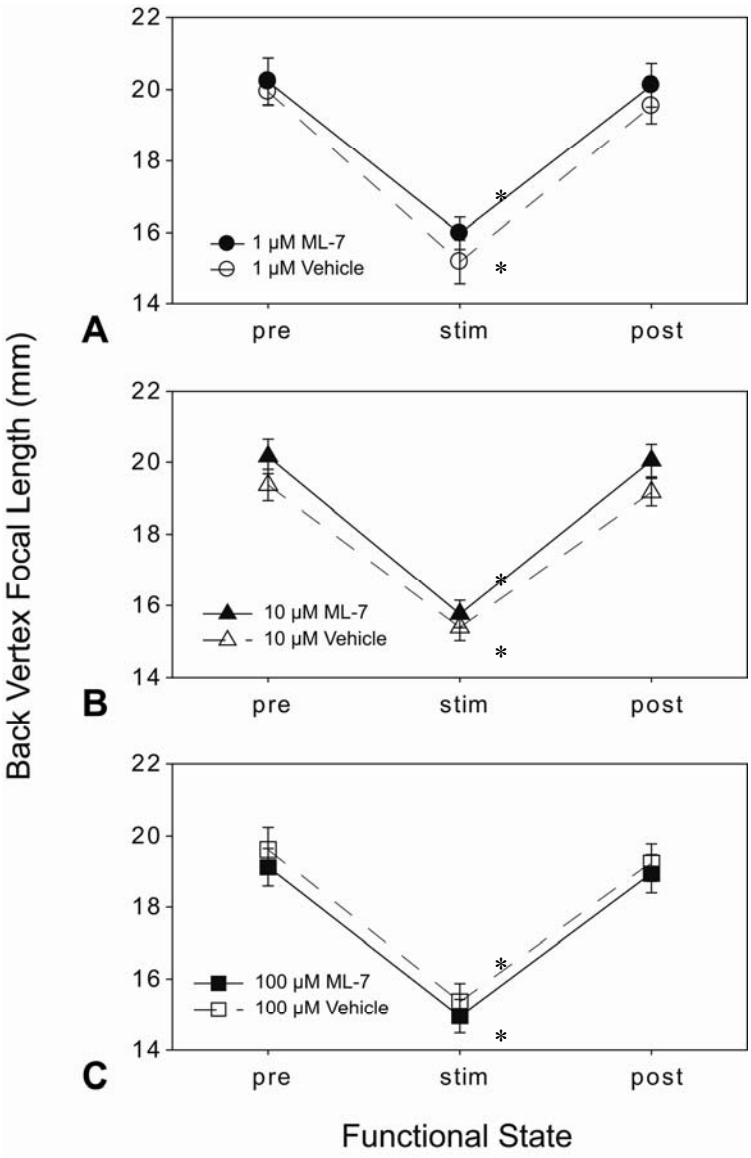

Figure 5: Line graphs showing the mean back vertex focal lengths (± s.e.m) for lenses treated with vehicle and ML-7 without a wash. A: 1 µM (n=4), B; 10 µM (n=12) C: 100 µM (n=9). For all three groups focal lengths for the stimulation state were significantly shorter that those at rest ($p < 0.0001$) which are denoted by asterisks.

Table 5: Back vertex focal length range and mean (± s.e.m) for each functional state for lenses treated with vehicle and ML-7 without a wash

Group	Focal length ranges (mm) and mean focal lengths ± s.e.m (mm) in parenthesis for each functional state of accommodation					
	Vehicle Treated Eyes			ML-7 Treated Eyes		
	Pre	Stim	Post	Pre	Stim	Post
1 μM (n=4)	19.13-22.17 (21.10 ± 0.68)	16.32 19.24 (17.68 ± 0.61)	19.00-22.10 (21.06 ± 0.73)	17.67-20.90 (20.01 ± 0.78)	14.08-18.78 (16.85 ± 1.08)	17.67-22.28 (20.53 ± 1.00)
10 μM (n=12)	17.87-20.62 (19.36 ± 0.44)	13.83-17.99 (15.34 ± 0.37)	16.63-21.73 (19.16 ± 0.39)	17.35-22.95 (20.16 ± 0.48)	13.62-17.73 (15.76 ± 0.39)	17.61-23.01 (20.04 ± 0.45)
100 μM (n=9)	17.52-22.16 (19.62 ± 0.62)	12.65-17.16 (15.37 ± 0.51)	17.24-22.04 (19.25 ± 0.54)	16.95-19.79 (19.12 ± 0.54)	12.33-15.73 (15.00 ± 0.48)	16.67-19.79 (19.00 ± 0.54)

post-stimulation state BVFLs jumped back to 19.25 ± 0.54 mm for the ML-7-treated eyes and 19.00 ± 0.54 mm for vehicle-treated eyes.

Although the overall effects were not significant, the following trend was observed: Eyes treated with vehicle in the 1 μM group showed slightly, although not always longer BVFLs in all three physiological states (pre-stimulation, stimulation, post-stimulation: p=0.02591, p=0.2281 and p=0.8945, respectively; Tukey; Figure 5a). This same trend was observed for the 10 μM group (p= 0.0013, p= 0.6407, p= 0.0004, respectively; Tukey; Figure 5b). In contrast, vehicle-treated eyes in the 100 μM group had slightly but not significantly longer back vertex distances in all three physiological states compared to the ML-7-treated eyes (pre-stimulation, stimulation, post-stimulation: p=0.3823, p=0.7276 and p=0.9627, respectively; Tukey; Figure 5c). The same pattern was observed in the 100 μM for the wash experiment.

The conversion of BVFLs and statistical analyses were done in the same manner as for the wash experiment. Two-way repeated measures analysis confirmed no significant differences between dosage groups and inhibition treatments (p=0.1428; Figure 6). Note that the 1 µM dosage group showed the same trend as all dosage groups in the wash experiment (vehicle-treated eyes having higher accommodation compared to ML-7-treated eyes), which the 1 µM and 10 µM did not.

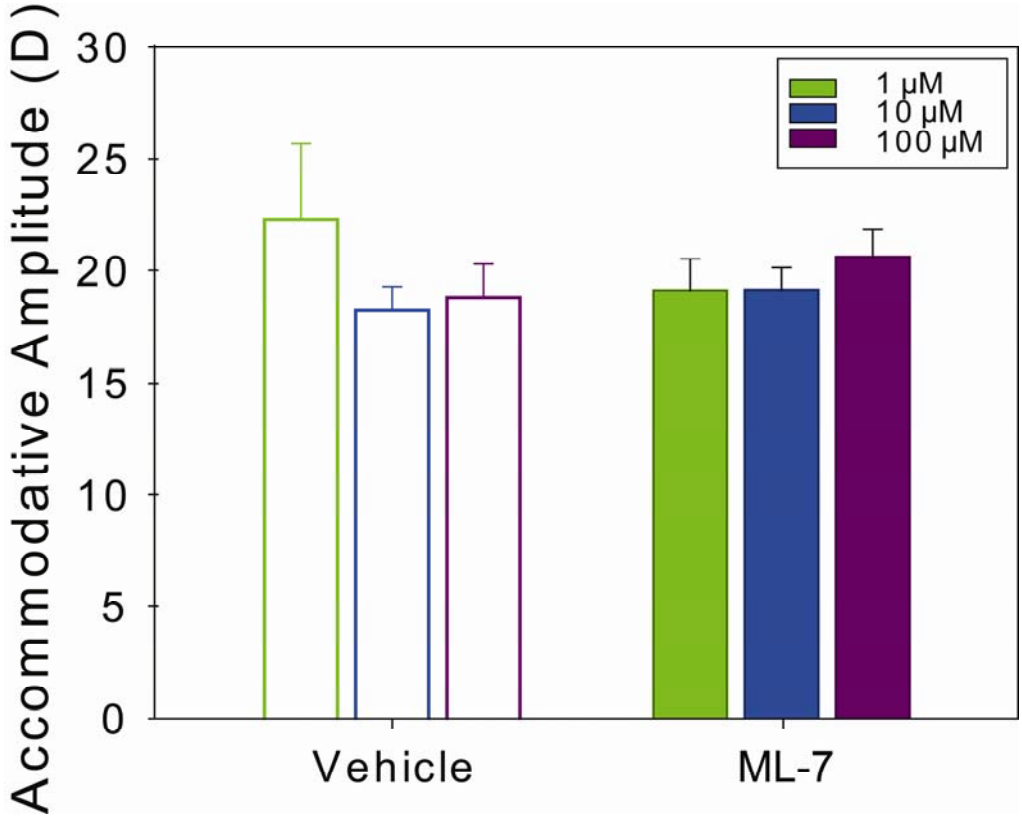

Figure 6: Bar graph showing accommodative amplitudes (± s.e.m) of vehicle and ML-7 treated eyes with no wash for all three dosage groups 1 µM (n=4), 10 µM (n=12) and 100 µM (n=9).

4.1.3 Overall effects

Although no interactions were detected between interocular differences in accommodative amplitude and dosage groups for both experiments (p=0.3294; Figure 7), the following trend was observed: The interocular differences for the no-wash experiment

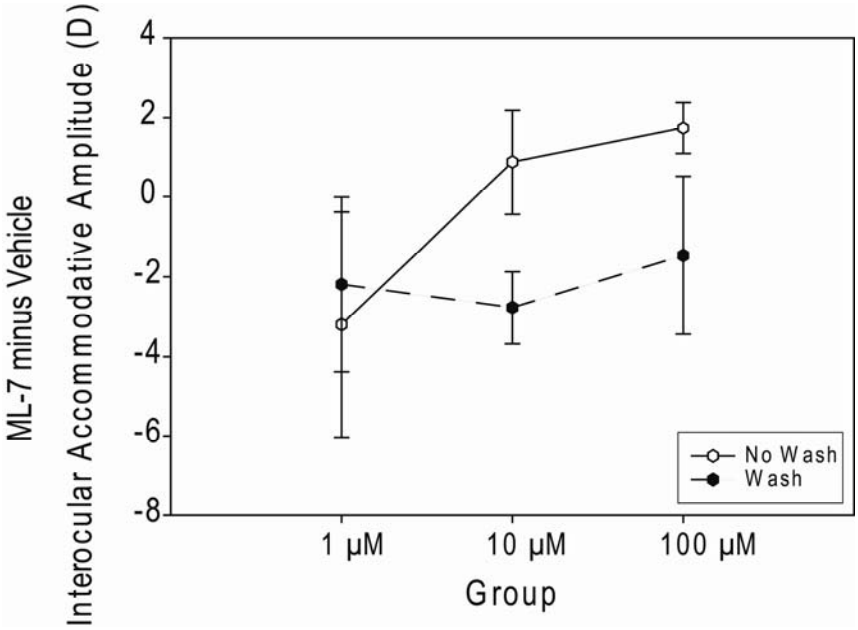

Figure 7: Line graph showing the interocular accommodative amplitudes (± s.e.m) for all three dosage (1 µM, 10 µM and 100 µM) groups for both experiments (wash and no-wash).

increased with increasing ML-7 concentrations (p=0.1428). For the wash experiment, this trend was not as obvious (p=0.8077). However, when collectively grouping the interocular differences by experiment, a significant difference was detected between the wash and no wash experiments (p=0.0159; Figure 8).

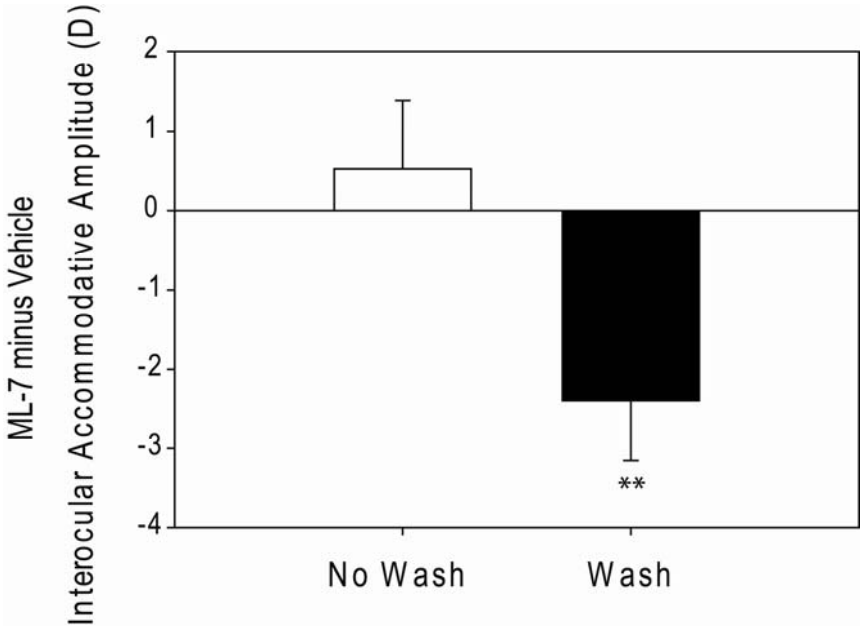

Figure 8: Bar graph showing the mean interocular accommodative amplitudes (± s.e.m) for the no-wash and wash experiments. The mean accommodative amplitude for the wash experiment was significantly lower than the no-wash experiment (p=0.0159) denoted by a double asterisks.

4.2 Detection of Phosphorylated Myosin

4.2.1 No-wash experiment (1 μM, 10 μm and 100 μM dosage groups)

Eyes treated with the ML-7 inhibitor showed less protein expression compared to their fellow vehicle-treated eyes, which showed greater protein expression in every dosage group (Figure 9).

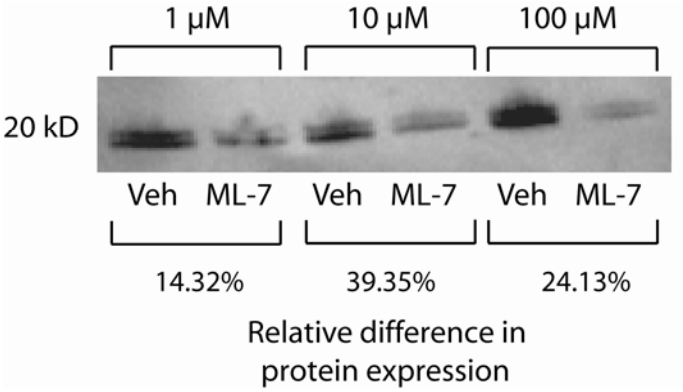

Figure 9: Western blot showing the amount of phosphorylated myosin for all dosage groups for the no-wash experiment. Eyes were treated with 1 µM, 10 µM and 100 µM of vehicle and ML-7. Relative difference in protein expression normalized relative to the vehicle-treated eye.

4.2.2 Wash versus no-wash (10 µM dosage group

Eyes that were washed after treatment had an overall lower percentage of protein expression (normalized relative to vehicle) and showed greater variability in protein expression (Figure 10) compared to eyes that were not washed. These differences in protein expression are summarised in Table 6. These results indicate that for the wash experiment, the average amount of phosphorylated myosin for eyes treated with ML-7 is 3.33% more than for eyes treated with vehicle. For the no-wash experiment, there was an average of 8.82% more phosphorylated protein measured from eyes treated with ML-7 compared to eyes treated with vehicle.

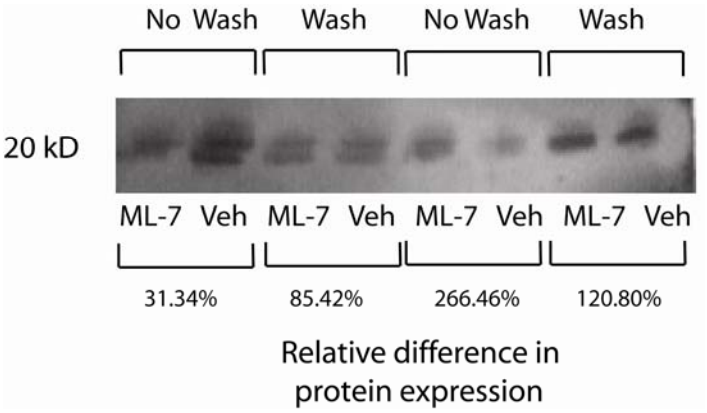

Figure 10: Representative Western blot showing the amount of phosphorylated myosin for eyes treated with 10 µM vehicle and ML-7 for both the wash and no-wash experiments. Relative difference in protein expression normalized relative to the vehicle-treated eyes.

Table 6: Mean relative difference of protein expression for the 10 µM dosage group for eyes treated with and without a wash.

Mean relative difference ± s.e.m for the amount of protein expression normalized to the vehicle-treated eye for the 10 µM dosage group	
Wash	**No Wash**
103.33 ± 10.22	108.82 ± 45.98
n = 3	n = 5

V. Discussion

5.1 Effects of ML-7

This is the first experiment to actively test the function of the cytoplasmic filaments on the lens during avian accommodation. The objective of this project was to determine whether the contractile microfilaments found on the lens contribute to accommodation. It was initially thought that when the microfilaments contract at the surfaces they would (along with the ciliary muscle) cause a decrease in radial curvature resulting in an increase in refractive power. In this experiment, ML-7 was used because it is a MLCK inhibitor and MLCK has been detected on the lens. Therefore, ML-7 was expected to disrupt any potential actin-myosin interactions occurring on the lens during accommodation. Eyes treated with ML-7 were expected to show a difference in accommodation compared to eyes treated with vehicle.

As previously shown, eyes were able to successfully accommodate by electrically inducing the ciliary nerve. The accommodative amplitudes obtained from the wash experiment were similar to results recorded from 7 day old chickens present in the study conducted by Choh *et al*. (2002). These values are also comparable to amplitudes found from the work of Glasser *et al*. (1995). Accommodative amplitudes for both vehicle- and ML-7-treated eyes from the no-wash experiment were slightly higher compared to values found in the literature. A possible explanation could be due to improvements with experimental techniques. More experience could have resulted in better dissections as well as a better connection of the stimulus electrode to the ciliary nerve consequently leading to maximal accommodation.

Although no differences in accommodative amplitudes were detected between vehicle- and ML-7-treated eyes, observations of the trends of the individual experiments (Figures 4 and 6) demonstrated that interfering with the surrounding environment by means of exposing the eye to an aqueous solution containing an MLCK inhibitor, had a subtle effect on accommodation. Washing the inhibitor also resulted in a difference between accommodative amplitudes, indicating another effect from interfering with the surrounding environment.

In the wash experiment, all three dosage groups treated with vehicle had higher accommodative amplitudes compared to eyes treated with ML-7 (Figure 4). This trend corresponded nicely to the original hypothesis that ML-7-treated eyes would be affected. Reviewing the literature on the uses of ML-7 revealed that its effects were reversible (Zhou and Cohan, 2001; Wong *et al.*, 2007). To eliminate this factor, the second experiment without the (3×10 min) wash was conducted.

The results were not the same for the wash and no-wash experiments. In the no-wash experiment, only the 1 μM dosage group showed similar results to the wash experiment (Figure 6). The 10 μM and 100 μM groups showed slightly higher accommodative amplitudes for eyes treated with ML-7 compared to their fellow vehicle-treated eyes. The 10 μM and 100 μM groups from the wash experiment showed an opposite trends with vehicle-treated eyes having longer accommodative amplitudes compared to eyes treated with ML-7. The results from this experiment indicate that the wash had an effect on the inhibition properties of ML-7.

To further investigate ML-7 activity, immunoblotting was carried out to detect the inhibition of MLCK by ML-7. Initially, a Western blot for all three dosage groups (no-wash

experiment) indicated that the inhibitor was working as suspected (Figure 9). However, when comparing the wash versus no-wash experiment, for just the 10 μM group, results showed greater variability (Figure 10). For the wash experiment, eyes showed an average relative difference of 103.33 ± 10.22 (s.e.m) whereas eyes treated without the wash had a slightly greater average relative difference of 108.82 ± 45.98 (s.e.m) (Table 6). These results revealed that some lenses treated with ML-7 showed a greater amount of phosphorylated myosin compared to their fellow vehicle-treated eyes and in some cases, the reverse. Results from these Western blots proved that MLCK inhibition was not consistent. A possible explanation could be with regards to the preparation of the samples. When carrying out these experiments, a large number of eyes were used. Removing the capsule, as well as storing the proteins on ice while waiting for the other samples to be completed, could have interfered with the inhibitory properties of ML-7. It was impossible for samples to be dissected and treated at the exact same time; variation in experimental times could have resulted in a difference in inhibitory function of the ML-7. The accommodation experiments also revealed the effectiveness of ML-7.

For both experiments, it was observed that in some birds the ML-7-treated eye accommodated better than the vehicle-treated eye and vice-versa. Both of the experimental paradigms (scans and Western blots) indicate inconsistencies in ML-7 activity.

Analysis of interocular differences for both experiments detected a difference between the wash and no-wash experiment. All ML-7-treated eyes (1 μM, 10 μM and 100 μM) followed by a (3×10 min) wash had significantly lower interocular differences compared to eyes treated with ML-7 and no wash (Figure 8). These findings show that ML-7 behaves differently when washed out. This could be due to the possible lingering effects of

ML-7 that seems to be occurring in the no-wash situation. For the wash experiment, it is apparent that the BVFL values for the 1 μM and 10 μM groups for both ML-7- and vehicle-treated eyes are similar at rest (Figures 3a and 3b). This is different compared to the no-wash experiment, where BVFLs from the 1 μM and 10 μM groups have ML-7-treated eyes starting at a higher BVFL at the pre-stimulation state than vehicle-treated eyes (Figures 5a and 5b).

For the 100 μM groups for both experiments, vehicle-treated eyes start off with higher BVFLs compared to the ML-7-treated eyes. It seems that higher concentrations of ML-7 have a unique and consistent effect. Lack of differences between the 100 μM groups might indicate that not enough ML-7 is being washed out. A possible explanation for this trend could be due to a phenomenon known as hormesis. Hormesis is an evolutionary adaptive response where a biological system ensures homeostasis is maintained (Calabrese and Baldwin, 2002). Hormesis is explained in toxicology as follows: low-dosages of treatment results in stimulation while high-levels of dosages results in inhibition (Calabrese, 2008). Since, in this experiment, the toxicological treatment is an inhibitor, it would be described as low-dose inhibition and high-dose non-inhibition. The actual mechanism of the hormesis phenomenon is controversial, however, it has been observed in a number of scientific papers (Calabrese and Baldwin, 2002; Chapman, 2002).

5.2 Future work

The results seem to confirm that ML-7 effects are highly reversible. In order to understand the effects of ML-7, a time lapse study would determine the time it takes for ML-7 to have an effect. For this particular experimental design, this would involve eyes being placed in the scanner with ML-7. BVFLs would be measured at different time

intervals to determine the changes in optical function. Note that a constant supply of oxygen would need to exist to ensure ciliary nerve health.

A possibility for inconsistent ML-7 activity might be related to the method of dissolving the ML-7 into an aqueous solution. US Biological Company recommends that ML-7 be solublized with hot ethanol and methanol whereas Sigma-Aldrich suggests solubilizing the powder with 50% water and 50% ethanol and no emphasis on temperature. Therefore, testing these two different methods may result in more inconsistent results.

It is known that most kinase inhibitors are reversible in nature, however, this can be reduced by using a more potent inhibitor as well as constantly keeping the eye in the presence of the inhibitor. Potency of an inhibitor can be measured by its half maximal inhibitory concentration (IC_{50}). IC_{50} is a quantitative value that measures the effectiveness of a chemical in inhibiting a biological function by half (Hoetelmans, 2000). Kinase inhibitors with specificities to MLCK showed to have IC_{50} values ranging from 0.0013 to 150. ML-7 is considered a potent inhibitor because it has a low IC_{50} value of 0.3, as well as it is specific to MLCK (Biomol, 2006).

To test inhibition while immunoblotting, a variant with the Western blot process would include the addition of ML-7 to buffers used for the dissections. Another modification would involve exposing the eye constantly to ML-7 which would eliminate the reversible effect of ML-7. In fact, a pilot study (n=3) was conducted to eliminate the reversible factor of ML-7. The purpose of this experiment was to investigate the effects of continuous exposure of ML-7 to chicken lenses with 100 μM of ML-7. After 15 minutes of treatment eyes were placed into the Scantox® and then connected to the electrode. The solution used for the Scantox® also contained 100 μM of inhibition treatment (ML-7 or vehicle). This

experiment assured that the eyes were continually in the presence of the inhibitor. The results indicate that ML-7-treated eyes had better accommodating abilities compared to eyes treated with vehicle (Figure 11). These results are similar to those of the no-wash experiment. The use of lower concentrations would be needed to test if a hormesis phenomenon is taking place. This experiment should be taken into consideration for further studies involving ciliary nerve induced accommodation and reversible inhibitors.

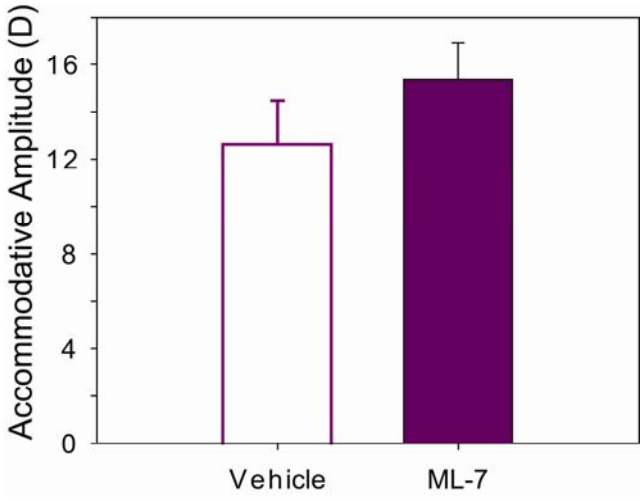

Figure 11: Bar graph showing accommodative amplitude of eyes treated with 100 µM vehicle and ML-7.

Another possibility would be to use a non-reversible inhibitor. In 2001, Hashimoto and Nonomura found a fungal strain, *Talaromyces wortmannin* KY12420, that was capable of producing a very potent irreversible MLCK inhibitor (Nakanishi *et al.*, 1992). The kinase inhibitor KY12420 would fit this experimental design because the concern of reversing the effects of inhibition would be eliminated. This would eliminate inconsistencies in immunoblots because there would be constant inhibition. However, this inhibitor may not be

ideal because it is highly toxic and could possibly affect the lens and surrounding structures, in particular the accommodative apparatus.

5.3 Conclusion

The use of ML-7 as a myosin light chain kinase inhibitor was not effective in this particular experimental design. Some of the results indicate that that ML-7 is ineffective at investigating any potential contractile microfilaments within the lens during accommodation. However, the findings of this study could not rule out a contractile system within the lens. Other strategies for detecting and evaluating the role of the cytoplasmic actin and myosin found within the lens include using a non-reversible inhibitor or ensuring constant exposure of the lens to a reversible inhibitor. Therefore, further investigation is needed to determine the role of contractile microfilaments during avian accommodation.

References

Al-Ghoul, K.J., Kirk, T., Kuszak, A.J., Zoltoski, R.K., Shiels, A. & Kuszak, J.R. (2003) Lens structure in MIP-deficient mice. *Anat Rec A Discov Mol Cell Evol Biol,* **273,** 714-730.

Azuma, M., Inoue, E., Oka, T. & Shearer, T.R. (1995) Proteolysis by calpain is an underlying mechanism for formation of sugar cataract in rat lens. *Curr Eye Res,* **14,** 27-34.

Bassnett, S., Missey, H. & Vucemilo, I. (1999) Molecular architecture of the lens fiber cell basal membrane complex. *J Cell Sci,* **112 (Pt 13),** 2155-2165.

Bhadriraju, K., Elliott, J.T., Nguyen, M. & Plant, A.L. (2007) Quantifying myosin light chain phosphorylation in single adherent cells with automated fluorescence microscopy. *BMC Cell Biol,* **8,** 43.

Bhatnagar, A., Ansari, N.H., Wang, L., Khanna, P., Wang, C. & Srivastava, S.K. (1995) Calcium-mediated disintegrative globulization of isolated ocular lens fibers mimics cataractogenesis. *Exp Eye Res,* **61,** 303-310.

Biomol, I. (2006) Specificities of Selected Ser/Thr Kinase Inhibitors, Vol. 2009, pp. Online Catalogue.

Bito, L.Z., Kaufman, P.L., DeRousseau, C.J. & Koretz, J. (1987) Presbyopia: an animal model and experimental approaches for the study of the mechanism of accommodation and ocular ageing. *Eye,* **1 (Pt 2),** 222-230.

Bloemendal, H. (1977) The vertebrate eye lens. *Science,* **197,** 127-138.

Bloemendal, H., de Jong, W., Jaenicke, R., Lubsen, N.H., Slingsby, C. & Tardieu, A. (2004) Ageing and vision: structure, stability and function of lens crystallins. *Prog Biophys Mol Biol,* **86,** 407-485.

Brown, N.A.P. & Bron, A.J. (1996) *Lens disorders : a clinical manual of cataract diagnosis,* Butterworth-Heinemann, Oxford ; Boston.

Calabrese, E. (2008) Hormesis and ethics: introduction. *Hum Exp Toxicol,* **27,** 601-602.

Calabrese, E.J. & Baldwin, L.A. (2002) Defining hormesis. *Hum Exp Toxicol,* **21,** 91-97.

Chapman, P.M. (2002) Defining hormesis: comments on Calabrese and Baldwin (2002). *Hum Exp Toxicol,* **21,** 99-101; discussion 113-104.

Charman, W.N. (2008) The eye in focus: accommodation and presbyopia. *Clin Exp Optom,* **91,** 207-225.

Chepelinsky, A.B. (2009) Structural function of MIP/aquaporin 0 in the eye lens; genetic defects lead to congenital inherited cataracts. *Handb Exp Pharmacol***,** 265-297.

Choh, V., Sivak, J.G. & Meriney, S.D. (2002) A physiological model to measure effects of age on lenticular accommodation and spherical aberration in chickens. *Invest Ophthalmol Vis Sci,* **43,** 92-98.

Cohen, A.I. (1965) The Electron Microscopy of the Normal Human Lens. *Invest Ophthalmol,* **4,** 433-446.

Donaldson, P., Kistler, J. & Mathias, R.T. (2001) Molecular solutions to mammalian lens transparency. *News Physiol Sci,* **16,** 118-123.

Dryer, S.E. (1994) Functional development of the parasympathetic neurons of the avian ciliary ganglion: a classic model system for the study of neuronal differentiation and development. *Prog Neurobiol,* **43,** 281-322.

Duane, A. (1925) Are the current theories of accommodation correct? *Am J Ophthalmol,* **8,** 196.

Fagerholm, P.P., Philipson, B.T. & Lindstrom, B. (1981) Normal human lens - the distribution of protein. *Exp Eye Res,* **33,** 615-620.

Fernald, R.D. & Wright, S.E. (1985) Growth of the visual system in the African cichlid fish, Haplochromis burtoni. Accommodation. *Vision Res,* **25,** 163-170.

Gao, J., Sun, X., Yatsula, V., Wymore, R.S. & Mathias, R.T. (2000) Isoform-specific function and distribution of Na/K pumps in the frog lens epithelium. *J Membr Biol,* **178,** 89-101.

Gilbert, S.F. (1994) *Developmental biology,* Sinauer Associates, Sunderland, Mass.
Glasser, A., Murphy, C.J., Troilo, D. & Howland, H.C. (1995) The mechanism of lenticular accommodation in chicks. *Vision Res,* **35,** 1525-1540.

Gwon, A. (2006) Lens regeneration in mammals: a review. *Surv Ophthalmol,* **51,** 51-62.
Helmholtz, H.v. & Southall, J.P.C. (1962) *Helmholtz's treatise on physiological optics,* Dover Publications, New York,.

Henze, M.J., Schaeffel, F., Wagner, H.J. & Ott, M. (2004) Accommodation behaviour during prey capture in the Vietnamese leaf turtle (Geoemyda spengleri). *J Comp Physiol A Neuroethol Sens Neural Behav Physiol,* **190,** 139-146.

Hightower, K.R., Leverenz, V. & Reddy, V.N. (1980) Calcium transport in the lens. *Invest Ophthalmol Vis Sci,* **19,** 1059-1066.

Hoenders, H.J. & Bloemendal, H. (1983) Lens proteins and aging. *J Gerontol,* **38,** 278-286.

Hoetelmans, R. (2000) PK-PD relationships for antiretroviral drugs, Vol. 2009. U.S. Food and Drug Administration, Silver Spring MD.

Ikeda, A. & Zwaan, J. (1967) The changing cellular localization of alpha-crystallin in the lens of the chicken embryo, studied by immunofluorescence. *Dev Biol,* **15,** 348-367.

Korn, E.D. (1978) Biochemistry of actomyosin-dependent cell motility (a review). *Proc Natl Acad Sci U S A,* **75,** 588-599.

Krag, S. & Andreassen, T.T. (2003) Mechanical properties of the human posterior lens capsule. *Invest Ophthalmol Vis Sci,* **44,** 691-696.

Kuszak, J.R., Ennesser, C.A., Umlas, J., Macsai-Kaplan, M.S. & Weinstein, R.S. (1988) The ultrastructure of fiber cells in primate lenses: a model for studying membrane senescence. *J Ultrastruct Mol Struct Res,* **100,** 60-74.

Kuszak, J.R., Mazurkiewicz, M., Jison, L., Madurski, A., Ngando, A. & Zoltoski, R.K. (2006) Quantitative analysis of animal model lens anatomy: accommodative range is related to fiber structure and organization. *Vet Ophthalmol,* **9,** 266-280.

Kuszak, J.R., Peterson, K.L. & Brown, H.G. (1996) Electron microscopic observations of the crystalline lens. *Microsc Res Tech,* **33,** 441-479.

Kuszak, J.R., Peterson, K.L., Sivak, J.G. & Herbert, K.L. (1994) The interrelationship of lens anatomy and optical quality. II. Primate lenses. *Exp Eye Res,* **59,** 521-535.

Kuszak, J.R., Zoltoski, R.K. & Sivertson, C. (2004a) Fibre cell organization in crystalline lenses. *Exp Eye Res,* **78,** 673-687.

Kuszak, J.R., Zoltoski, R.K. & Tiedemann, C.E. (2004b) Development of lens sutures. *Int J Dev Biol,* **48,** 889-902.

Kuwabara, T. (1975) The maturation of the lens cell: a morphologic study. *Exp Eye Res,* **20,** 427-443.

Lewis, S.A. & Donaldson, P. (1990) Ion Channels and Cell Volume Regulation: Chaos in an Organized System. *News Physiol Sci,* **5,** 112-119.

Lovicu, F.J. & Robinson, M.L. (2004) *Development of the ocular lens,* Cambridge University Press, Cambridge, UK ; New York.

Mach, H. (1963) [Investigations on Lens Protein and Microelectrophoresis of Hydrosoluble Protein in Senile Cataract.]. *Klin Monatsbl Augenheilkd,* **143,** 689-710.

Magid, A.D., Kenworthy, A.K. & McIntosh, T.J. (1992) Colloid osmotic pressure of steer crystallins: implications for the origin of the refractive index gradient and transparency of the lens. *Exp Eye Res,* **55,** 615-627.

Mathias, R.T. & Rae, J.L. (1985) Transport properties of the lens. *Am J Physiol,* **249,** C181-190.

Mathias, R.T. & Rae, J.L. (2004) The lens: local transport and global transparency. *Exp Eye Res,* **78,** 689-698.

Mathias, R.T., Rae, J.L. & Baldo, G.J. (1997) Physiological properties of the normal lens. *Physiol Rev,* **77,** 21-50.

McAvoy, J.W. (1978a) Cell division, cell elongation and distribution of alpha-, beta- and gamma-crystallins in the rat lens. *J Embryol Exp Morphol,* **44,** 149-165.

McAvoy, J.W. (1978b) Cell division, cell elongation and the co-ordination of crystallin gene expression during lens morphogenesis in the rat. *J Embryol Exp Morphol,* **45,** 271-281.

McDevitt, D.S., Meza, I. & Yamada, T. (1969) Immunofluorescence localization of the crystallins in amphibial lens development, with special reference to the gamma-crystallins. *Dev Biol,* **19,** 581-607.

Merriman-Smith, R., Donaldson, P. & Kistler, J. (1999) Differential expression of facilitative glucose transporters GLUT1 and GLUT3 in the lens. *Invest Ophthalmol Vis Sci,* **40,** 3224-3230.

Murphy, C.J., Glasser, A. & Howland, H. (1995) The anatomy of the ciliary region of the chicken eye. *Invest Ophthalmol,* **36,** 886-896.

Nakanishi, S., Kakita, S., Takahashi, I., Kawahara, K., Tsukuda, E., Sano, T., Yamada, K., Yoshida, M., Kase, H., Matsuda, Y. & et al. (1992) Wortmannin, a microbial product inhibitor of myosin light chain kinase. *J Biol Chem,* **267,** 2157-2163.

Obrecht, G.r. & Stark, L. (1991) *Presbyopia research : from molecular biology to visual adaptation,* Plenum Press, New York.

Oriowo, O.M. (2003) AlamarBlue bioassay for cellular investigation of UV-induced crystalline lens damage. *Ophthalmic Physiol Opt,* **23,** 307-314.

Ott, M. (2006) Visual accommodation in vertebrates: mechanisms, physiological response and stimuli. *J Comp Physiol A Neuroethol Sens Neural Behav Physiol,* **192,** 97-111.

Oyster, C.W. (1999) *The human eye : structure and function,* Sinauer Associates, Sunderland, Mass.

Paterson, C.A., Zeng, J., Husseini, Z., Borchman, D., Delamere, N.A., Garland, D. & Jimenez-Asensio, J. (1997) Calcium ATPase activity and membrane structure in clear and cataractous human lenses. *Curr Eye Res,* **16,** 333-338.

Piatigorsky, J. (1981) Lens differentiation in vertebrates. A review of cellular and molecular features. *Differentiation,* **19,** 134-153.

Pierscionek, B.K. (1993) What we know and understand about presbyopia. *Clinical & Experimental Optometry,* **73.3,** 83-90.

Pollard, T.D. & Weihing, R.R. (1974) Actin and myosin and cell movement. *CRC Crit Rev Biochem,* **2,** 1-65.

Rabaey, M. (1965) Lens Proteins During Embryonic Development of Different Vertebrates. *Invest Ophthalmol,* **4,** 560-578.

Rafferty, N.S. & Goossens, W. (1978) Cytoplasmic filaments in the crystalline lens of various species: functional correlations. *Exp Eye Res,* **26,** 177-190.

Rafferty, N.S., Rafferty, K.A. & Ito, E. (1994) Agonist-induced rise in intracellular calcium of lens epithelial cells: effects on the actin cytoskeleton. *Exp Eye Res,* **59,** 191-201.

Rafferty, N.S. & Scholz, D.L. (1984) Polygonal arrays of microfilaments in epithelial cells of the intact lens. *Curr Eye Res,* **3,** 1141-1149.

Rafferty, N.S. & Scholz, D.L. (1985) Actin in polygonal arrays of microfilaments and sequestered actin bundles (SABs) in lens epithelial cells of rabbits and mice. *Curr Eye Res,* **4,** 713-718.

Rafferty, N.S. & Scholz, D.L. (1989) Comparative study of actin filament patterns in lens epithelial cells. Are these determined by the mechanisms of lens accommodation? *Curr Eye Res,* **8,** 569-579.

Rafferty, N.S., Scholz, D.L., Goldberg, M. & Lewyckyj, M. (1990) Immunocytochemical evidence for an actin-myosin system in lens epithelial cells. *Exp Eye Res,* **51,** 591-600.

Rao, P.V. & Maddala, R. (2006) The role of the lens actin cytoskeleton in fiber cell elongation and differentiation. *Semin Cell Dev Biol,* **17,** 698-711.

Remington, L.-A. (2005) *Clinical Anatomy of the visual system*.

Rosenthal, R., Choritz, L., Schlott, S., Bechrakis, N.E., Jaroszewski, J., Wiederholt, M. & Thieme, H. (2005) Effects of ML-7 and Y-27632 on carbachol- and endothelin-1-induced contraction of bovine trabecular meshwork. *Exp Eye Res,* **80,** 837-845.

Sanderson, J., Marcantonio, J.M. & Duncan, G. (1996) Calcium ionophore induced proteolysis and cataract: inhibition by cell permeable calpain antagonists. *Biochem Biophys Res Commun,* **218,** 893-901.

Scammon, R. & Hesdorffer, M. (1937) Growth in mass and volume of the human lens in postnatal life. *Archives of Ophthalmology,* **17,** 104-112.

Schaeffel, F., Murphy, C.J. & Howland, H.C. (1999) Accommodation in the cuttlefish (Sepia officinalis). *J Exp Biol,* **202,** 3127-3134.

Schwartz, S.H. (1994) *Visual perception : a clinical orientation,* Appleton & Lange, Norwalk, Conn.

Shubert, E.E., Trevithick, J.R. & Hollenberg, M.J. (1970) Localization of gamma crystallins in the developing lens of the rat. *Can J Ophthalmol,* **5,** 353-365.

Sigma-Aldrich (2009) 1-(5-Chloronaphthalene-1-sulfonyl)-1H-hexahydro-1,4-diazepine hydrochloride, Vol. 2009.

Silverthorn, D.U. (2004) *Human physiology : an integrated approach,* Pearson/Benjamin Cummings, San Francisco.

Sivak, J.G. (2008) The role of the lens in refractive development of the eye: animal models of ametropia. *Exp Eye Res,* **87,** 3-8.

Sivak, J.G., Hildebrand, T. & Lebert, C. (1985) Magnitude and rate of accommodation in diving and nondiving birds. *Vision Res,* **25,** 925-933.

Sivak, J.G., Hildebrand, T.E., Lebert, C.G., Myshak, L.M. & Ryall, L.A. (1986) Ocular accommodation in chickens: corneal vs lenticular accommodation and effect of age. *Vision Res,* **26,** 1865-1872.

Spudich, J.A., Huxley, H.E. & Finch, J.T. (1972) Regulation of skeletal muscle contraction. II. Structural studies of the interaction of the tropomyosin-troponin complex with actin. *J Mol Biol,* **72,** 619-632.

Tian, B., Brumback, L.C. & Kaufman, P.L. (2000) ML-7, chelerythrine and phorbol ester increase outflow facility in the monkey Eye. *Exp Eye Res,* **71,** 551-566.

Tsonis, P.A. & ScienceDirect (Online service) (2008) Animal models in eye research, pp. xiv, 215 p. Academic Press, San Diego.

van de Kamp, M. & Zwann, J. (1973) Intracellular localization of lens antigens in the developing eye of the mouse embryo. *J Exp Zool,* **186,** 23-32.

Vrensen, G.F. (2009) Early cortical lens opacities: a short overview. *Acta Ophthalmol,* **87,** 602-610.

Walls, G.L. (1963) *The vertebrate eye and its adaptive radiation,* Hafner Pub. Co., New York.

Willekens, B. & Vrensen, G. (1985) Lens fiber organization in four avian species: a scanning electron microscopic study. *Tissue Cell,* **17,** 359-377.

Wong, R., Fabian, L., Forer, A. & Brill, J.A. (2007) Phospholipase C and myosin light chain kinase inhibition define a common step in actin regulation during cytokinesis. *BMC Cell Biol,* **8,** 15.

Zhou, F.Q. & Cohan, C.S. (2001) Growth cone collapse through coincident loss of actin bundles and leading edge actin without actin depolymerization. *J Cell Biol,* **153,** 1071-1084.

Zwaan, J. & Ikeda, A. (1968) Macromolecular events during differentiation of the chicken lens. *Exp Eye Res,* **7,** 301-311.